The negative adipogenesis regulator DLK1 is transcriptionally regulated by TIS7 (IFRD1) and translationally by its orthologue SKMc15 (IFRD2)

[1]Ilja Vietor*, [1,12]Domagoj Cikes, [1,13]Kati Piironen, [1,14]Ronald Gstir, [2]Matthias David Erlacher, [3]Michael Hess, [4]Volker Kuhn (†), [5]Gerald Degenhart, [6,7]Jan Rozman, [8,9,10]Martin Klingenspor, [6,7,11] Martin Hrabe de Angelis, [1]Taras Valovka, [1, 14]Lukas A. Huber

[1]Institute of Cell Biology, Biocenter, [2]Division of Genomics and RNomics, Biocenter, [3]Division of Histology and Embryology, [4]Department Trauma Surgery, [5]Department Radiology, Medical University Innsbruck, Austria, [6]German Mouse Clinic, Institute of Experimental Genetics, Helmholtz Zentrum München, German Research Center for Environmental Health, Neuherberg, Germany, [7]German Center for Diabetes Research (DZD), Neuherberg, Germany, [8]Chair of Molecular Nutritional Medicine, Technical University of Munich, School of Life Sciences, Weihenstephan, Freising, Germany, [9]EKFZ - Else Kröner Fresenius Center for Nutritional Medicine, Technical University of Munich, Freising, Germany, [10]ZIEL - Institute for Food & Health, Technical University of Munich, Freising, Germany, [11]Chair of Experimental Genetics, Technical University of Munich, School of Life Sciences, Weihenstephan, Freising, Germany, [12]IMBA, Institute of Molecular Biotechnology of the Austrian Academy of Sciences, Vienna, Austria, [13]Division of Pharmaceutical Chemistry and Technology, Faculty of Pharmacy, University of Helsinki, Finland, [14]ADSI – Austrian Drug Screening Institute GmbH, Innsbruck, Austria

* Address correspondence to: Ilja Vietor, Institute of Cell Biology, Biocenter, Innsbruck Medical University, Innrain 80-82, A-6020 Innsbruck, Austria. Phone: +43 512 9003 70175 E-mail: ilja.vietor@i-med.ac.at

† Deceased May 2019

Running title: Identification of novel regulators of adipogenesis

Conflict of interest: The authors declare that they have no conflict of interest.

Abstract

Delta-like homolog 1 (DLK1), an inhibitor of adipogenesis, controls the cell fate of adipocyte progenitors. Understanding regulatory mechanisms affecting DLK1 levels is therefore of high interest. Here we identify two independent mechanisms, transcriptional and translational, by which TIS7 (IFRD1) and its orthologue SKMc15 (IFRD2) regulate DLK1 levels. Mice deficient in both TIS7 and SKMc15 (dKO) had severely reduced adipose tissue and were resistant to high fat diet-induced obesity. Wnt signaling, a negative regulator of adipocyte differentiation was significantly up regulated in dKO mice. Elevated levels of the Wnt/β-catenin target protein Dlk-1 inhibited the expression of adipogenesis regulators PPARγ and C/EBPα, and fatty acid transporter CD36. Although both, TIS7 and SKMc15, contributed to this phenotype, they utilized two different mechanisms. TIS7 acted by controlling Wnt signaling and thereby transcriptional regulation of Dlk-1. On the other hand, here we provide experimental evidence that SKMc15 acts as a general translational inhibitor affecting DLK-1 protein levels. Our study provides data describing novel mechanisms of DLK1 regulation in adipocyte differentiation involving TIS7 and SKMc15.

26
27
28
29
30
31
32
33
34
35
36
37
38
39
40
41
42
43
44
45 *Nonstandard abbreviations used:* CD36, cluster of differentiation 36; HFD, high fat diet; IFRD, interferon
46 related developmental regulator; KO, knockout; dKO, double knockout; RD, regular diet; SKMc15, skeletal
47 muscle cDNA library clone15; TIS7, TPA Induced Sequence 7

48 **Introduction**

49 Adipogenesis is a complex process in which multipotent stem cells are converted into preadipocytes before
50 terminal differentiation into adipocytes [1]. These mechanisms involve protein factor regulators, epigenetic
51 factors, and miRNAs. TPA Induced Sequence 7 (TIS7) protein has been shown to be involved in the mainly
52 transcriptional regulation of differentiation processes in various cell types, e.g. neurons [2], enterocytes [3],
53 myocytes [4] and also adipocytes [5].

54 Multiple lines of evidence link the regulation of Wnt/β-catenin signaling to the physiological function of TIS7,
55 known in human as Interferon related developmental regulator 1 (IFRD1) [6, 7]. Our data based on experiments
56 with TIS7 knockout mice show a negative effect of TIS7 on Wnt signaling and a positive on adipocyte
57 differentiation [6, 8]. TIS7 deficiency leads to a significant up regulation of Wnt/β-catenin transcriptional activity
58 in both primary osteoblasts and in mouse embryonic fibroblasts (MEFs) derived from TIS7 knockout (KO)
59 mice. Recent data show that TIS7 is also involved in the control of adipocytes differentiation in mice and was
60 up regulated in both visceral (vWAT) and subcutaneous (sWAT) white adipose tissues (WAT) of genetically
61 obese ob/ob mice [5]. TIS7 transgenic mice have increased total body adiposity and decreased lean mass
62 compared with wild type (WT) littermates [3]. On HFD, TIS7 transgenic mice exhibit a more rapid and
63 proportionately greater gain in body weight with persistently elevated total body adiposity. Enhanced
64 triglyceride (TG) absorption in the gut of TIS7 transgenic mice [3] indicated that TIS7 expressed in the gut
65 epithelium has direct effects on fat absorption in enterocytes. We have shown that as a result of impaired
66 intestinal lipid absorption TIS7 KO mice displayed lower body adiposity [8]. Compared with WT littermates,
67 TIS7 KO mice do not gain weight when chronically fed an HFD and TIS7 deletion results in delayed lipid
68 absorption and altered intestinal and hepatic lipid trafficking, with reduced intestinal TG, cholesterol, and free
69 fatty acid mucosal levels in the jejunum [9]. TIS7 protein functions as a transcriptional co-regulator [10] due to its
70 interaction with protein complexes containing either histone deacetylases (HDAC) [4, 11, 12, 13] or protein methyl
71 transferases, in particular PRMT5 [14]. The analysis of adipocyte differentiation in preadipocytic 3T3-L1 cells
72 suggested an involvement of TIS7 in the regulation of adipogenesis in the Wnt/β-catenin signaling context [5].

73 SKMc15, also known as Interferon related developmental regulator 2 (IFRD2), a second member of TIS7
74 gene family, is highly conserved in different species [15]. Mouse TIS7 and SKMc15 are highly homologous,
75 with a remarkable identity at both the cDNA and amino acid levels (58% and 88%, respectively). However,
76 there was so far no information about the physiological function and mechanisms of action of SKMc15 and
77 its possible involvement in differentiation of various tissues. Recently, cryo-electronmicroscopy (cryo-EM)
78 analyses of inactive ribosomes identified IFRD2 (SKMc15) as a novel ribosome-binding protein inhibiting
79 translation to regulate gene expression [16]. The physiological function of SKMc15 matching the mechanism
80 based on the above mentioned cryo-EM data was so far not shown and we postulate it could be involved in
81 adipogenesis, since a significant reduction of whole protein synthesis was previously shown as a major
82 regulatory event during early adipogenic differentiation [17].
83 Adipogenesis occurs late in embryonic development and in postnatal periods. Adipogenic transcription
84 factors CCAAT/enhancer binding protein α (C/EBPα) and peroxisome proliferator activated receptor γ
85 (PPARγ) play critical roles in adipogenesis and in the induction of adipocyte markers [18]. PPARγ is the major
86 downstream target of Delta-like protein 1 (DLK-1). It is inactivated by the induction of the MEK/ERK pathway
87 leading to its phosphorylation and proteolytic degradation [19]. DLK-1, also known as Pref-1 (preadipocyte
88 factor 1) activates the MEK/ERK pathway to inhibit adipocyte differentiation [20]. C/EBPα is highly expressed
89 in mature adipocytes and can bind DNA together with PPARγ to a variety of respective target genes [21].
90 Besides that, PPARγ binding to C/EBPα gene induces its transcription, thereby creating a positive feedback
91 loop [22]. Both proteins have synergistic effects on the differentiation of adipocytes that requires a balanced
92 expression of both C/EBPα and PPARγ.
93 Wnt/β-catenin signaling is one of the extracellular signaling pathways specifically affecting adipogenesis [23,
94 24, 25] by maintaining preadipocytes in an undifferentiated state through inhibition of C/EBPα and PPARγ [26].
95 PPAR-γ and Wnt/β-catenin pathways are regarded as master mediators of adipogenesis [27]. Wnt signaling is
96 a progenitor fate determinator and negatively regulates preadipocyte proliferation through DLK-1 [28]. Mice
97 over-expressing DLK-1 are resistant to HFD-induced obesity, whereas DLK-1 KO mice have accelerated

98 adiposity [29]. DLK-1 transgenic mice show reduced expression of genes controlling lipid import (CD36) and
99 synthesis (Srebp1c, Pparγ) [30]. DLK-1 expression coincides with altered recruitment of PRMT5 and β-catenin
100 to the DLK-1 promoter [31]. PRMT5 acts as a co-activator of adipogenic gene expression and differentiation [32].
101 SRY (sex determining region Y)-box 9 (Sox9), a transcription factor expressed in preadipocytes, is down
102 regulated preceding adipocyte differentiation. DLK-1 prevents down regulation of Sox9 by activating ERK,
103 resulting in inhibition of adipogenesis [33]. The PRMT5- and histone-associated protein COPR5, affects PRMT5
104 functions related to cell differentiation [34]. Adipogenic conversion is delayed in MEFs derived from COPR5
105 KO mice and WAT of COPR5 KO mice is reduced when compared to control mice. DLK-1 expression is up
106 regulated in COPR5 KO cells [31].
107 Here we show the involvement of TIS7 and SKMc15 in the process of adipocyte differentiation. dKO mice
108 had strongly decreased amounts of the body fat when fed with even regular, chow diet and were resistant
109 against the high fat diet induced obesity. We found two independent molecular mechanisms through which
110 TIS7 and SKMc15 fulfill this function in a synergistic manner. TIS7 regulates the Wnt signaling pathway
111 activity and restricts DLK-1 protein levels, thereby allowing adipocyte differentiation. In contrast, SKMc15 KO
112 did not affect Wnt signaling, but as we show here, cells lacking SKMc15 have significantly up regulated
113 translational activity. This was true also for dKO, but not for the single TIS7 knockout cells. The ablation of
114 both TIS7 and SKMc15 genes significantly affected the expression of genes essential for adipocyte
115 differentiation and function. Since dKO mice render a substantially leaner phenotype on chow diet, even
116 without any challenge by HFD-induction, we propose that TIS7 and SKMc15 represent novel players in the
117 process of physiological adipocyte differentiation.
118
119 **Results**
120 *Mice lacking TIS7 and SKMc15 genes have lower body mass, less fat and are resistant against HFD-induced*
121 *obesity.*
122 In order to clarify whether both, TIS7 and SKMc15 are involved in the regulation of the adipocyte
123 differentiation and if they act through same or different mechanisms, we have generated mice lacking both

genes by crossing TIS7 with SKMc15 single KO mice. dKO pups were viable, and adult male and female mice were fertile. At birth, body weights of dKO and WT mice were similar. Nevertheless, already during weaning, both the male and female dKO mice failed to gain weight when compared to their WT littermates and this persisted in the following weeks when the mice were fed regular diet (RD; chow diet) containing 11 % kcal of fat. At 10 weeks of age, dKO mice displayed 30 % and later up to 44.9 % lower body weight compared with WT mice (Figure 1a).

Based on Dual Energy X-ray Absorptiometry (DEXA) measurement, 6-month-old WT mice had substantially higher amounts of fat than their dKO littermates (Figure 1b, left panel). The effect of TIS7 and SKmc15 double knockout was even more pronounced when the total fat and lean mass values were normalized to the body weight since the dKO mice were smaller than their WT counterparts. The percentage of fat was in the WT mice 37.7 ± 4 % vs. 6 ± 3 % of the total body mass in dKO animals. Furthermore, the percentage of lean tissue mass in WT animals was lower than in dKO animals (60 ± 4.6 % vs. 92 ± 3.14 %; Figure 1b, right panel). Nevertheless, the dKO mice were not overall smaller, since their body length, including the tail did not significantly differ between WT and dKO mice at different age (n=20; data not shown). Next, we analyzed the contribution of TIS7 and SKMc15 to the whole-body fat content of mice. Three-dimensional reconstruction of images based on micro-computed tomography (micro-CT) of sex/age-matched adult mice disclosed that both TIS7 and SKMc15 single KO mice already had less abdominal fat than WT controls and that the dKO of TIS7 and SKMc15 genes caused the strongest decrease in abdominal fat content and size (Figure 1c). Quantitative analyses of micro-CT measurements showed that TIS7 deficiency caused a substantial lack of the abdominal fat tissues (P=0.002 when compared to WT mice, Figure 2a). Whereas TIS7 KO mice had less fat mass but were not significantly lighter than their WT littermates (Figure 2b), SKMc15 KO were lighter (P=0.007) and leaner (P=0.0001) and dKO mice were both significantly lighter (P = 0.0001) and had significantly less abdominal fat (P=0.006) than the WT mice (Figures 2a, b).

We conducted an indirect calorimetry trial with sex- and age-matched WT and dKO animals (Supplementary figure 1). We did not identify any significant difference in respiratory exchange ratios (RER = VCO2/VO2) of

149 WT and dKO mice (Supplementary figure 1a). However, dKO mice showed substantially reduced body
150 weight, mainly because of lacking fat, despite identical food intake, activity and no major differences in several
151 metabolic parameters. To investigate potential links between TIS7, SKMc15 and obesity, we studied the
152 response of dKO mice to HFD. At 2 months of age, male mice were housed individually and fed with HFD for
153 21 days. Food intake was measured every second day and body weight was measured every fourth day.
154 Feces were collected every second day to analyze the composition of excreted lipids and blood samples
155 were collected after the third week of HFD feeding to measure the concentrations of hepatic and lipoprotein
156 lipases, respectively. Already within the first week of HFD feeding, WT mice gained more weight than the
157 dKO mice (Figure 2c), although there were no obvious differences in food consumption (Supplementary
158 figure 1b) or in levels of lipolytic enzymes (Supplementary figures 1c, d). These differences in body weight
159 gain continued to increase during the second and third week, at which time the body weight of WT mice
160 increased additionally for 30% (30.0 ± 2.3%) when compared with the beginning of the HFD feeding period.
161 In contrast, the weight of dKO animals increased only slightly (7.6 ± 1.6%) (Figure 2c). Both genes, TIS7 and
162 SKMc15 contributed to this phenotype and we could see an additive effect following their deletion (Figure
163 2c).

164 *Adipocyte differentiation in dKO mice is inhibited due to up regulated DLK-1 levels.*

165 A possible explanation of the lean phenotype of dKO mice was that TIS7 and SKMc15 regulate adipocyte
166 differentiation. Primary MEFs derived from totipotent cells of early mouse mammalian embryos are capable
167 of differentiating into adipocytes and they are versatile models to study adipogenesis as well as mechanisms
168 related to obesity such as genes, transcription factors and signaling pathways implicated in the adipogenesis
169 process [35]. To test whether TIS7 and SKMc15 are required for adipogenesis we treated MEFs derived from
170 WT, SKMc15 and TIS7 single and dKO mice using an established adipocyte differentiation protocol [36].
171 Expression levels of both TIS7 and SKMc15 mRNA increased during the adipocyte differentiation of WT
172 MEFs. TIS7 expression reached maximum levels representing 5.7-fold increase compared to proliferating
173 WT MEFs on day 3 and SKMc15 reached on day 5 the maximum of 2.5-fold expression levels of proliferating

174 MEFs (Supplementary figure 2). These data suggested that both proteins play a regulatory role in
175 adipogenesis, however differ in their mechanisms and timing. Eight days after initiation of adipocyte
176 differentiation a remarkable reduction of adipocyte differentiation potential in SKMc15, TIS7 KO MEFs and
177 dKO MEFs was observed, as characterized by the formation of lipid droplets stained by oil red O (Figure 3a).
178 Quantification of this staining revealed that fat vacuole formation in cells derived from SKMc15, TIS7 and
179 dKO mice represented 65 %, 35 % and 24 % of the WT cells, respectively (Figure 3b). These data indicated
180 that both, TIS7 and SKMc15 were critical for adipocyte differentiation and that the defect in adipogenesis
181 could be responsible for the resistance of dKO mice to HFD-induced obesity.
182 Wnt/β-catenin signaling is an important regulatory pathway for adipocyte differentiation [37]. Consistently,
183 others and we have shown that TIS7 deficiency causes up regulation of Wnt/β-catenin transcriptional activity.
184 Therefore, we have assessed Wnt signaling activity in MEFs by measuring transcriptional activity using
185 TOPflash, TCF-binding luciferase reporter assays. As shown in Figure 3c, Wnt signaling activity, when
186 compared to the WT MEFs, was not regulated in SKMc15 KO, but significantly up regulated in TIS7 KO
187 ($P<0.0001$) and also in dKO MEFs ($P<0.01$). Supporting these findings, Western blot analyses of WAT
188 samples also identified increased β-catenin protein levels in WAT of TIS7 KO and in dKO mice ($P<0.0001$),
189 but not in SKMc15 KO mice (Figure 3d, top panel) suggesting the involvement of TIS7 but not SKMc15 in
190 the Wnt signaling pathway regulation.
191 Next, we analyzed the expression levels of DLK-1, a negative regulator of adipogenesis and at the same
192 time known target of Wnt signaling [31]. DLK-1 protein was significantly upregulated in WAT isolated from TIS7
193 and SKMc15 KO as well as from dKO mice (Figure 3d, bottom panel). The qPCR analysis revealed a
194 significant up regulation of DLK-1 mRNA levels in dKO WAT samples ($P<0.01$) and similarly in dKO MEFs
195 ($P<0.05$) when compared to the WT controls (Figure 4a). Moreover, whereas in the WT MEFs the expression
196 of DLK-1 was strongly up regulated only during the first day of adipocyte differentiation and then over the
197 next days declined to basal levels, in dKO MEFs DLK-1 was up regulated ($P<0.001$) throughout the entire 8
198 days of differentiation (Figure 4b). This result was confirmed on the protein level by Western blot analyses of

199 lysates from 8 day differentiated adipocytes (Figure 4c). A rescue experiment was conducted to confirm that
200 DLK-1 expression was TIS7- and SKMc15-dependent. dKO MEFs were transiently co-transfected with TIS7
201 and SKMc15 vectors and 48 hours later the mRNA expressions were analyzed by RT-qPCR. Ectopic co-
202 expression of TIS7 and SKMc15 significantly ($P<0.05$) down regulated the DLK-1 expression (Figure 4d).
203 Accordingly, TIS7 and/or SKMc15 are involved in the regulation of DLK-1 expression, but the molecular
204 mechanism remained unclear.
205 Our earlier study revealed that TIS7 binds directly to DNA and via interaction with PRMT5 regulates gene
206 expression [14]. Therefore, we performed chromatin immunoprecipitation (ChIP) experiments where we
207 studied the binding of TIS7 and SKMc15 as well as known transcription factors (β-catenin and H4R3me2s
208 (symmetrically dimethylated histone H4 at arginine residue 3)) [31] to the regulatory elements of the DLK-1
209 gene. In dKO MEFs treated 8 days with the adipocyte differentiation cocktail we found increased β-catenin
210 binding to the β-catenin/TCF binding site 2 of the Dlk-1 regulatory element when compared to WT MEFs
211 (Figure 4e). On the other hand, binding of H4R3me2s to the same Dlk-1 regulatory element was significantly
212 reduced ($P<0.0001$). We could not identify any direct binding of TIS7 or SKMc15 proteins to two different
213 DLK-1 regulatory elements (Dlk-1 region A and β-cat/TCFbs2), neither in WT nor in dKO MEFs, suggesting
214 rather an epigenetic regulation than *via* their direct binding to DLK-1 regulatory elements. We concluded that
215 TIS7 and SKMc15 are required to restrain the DLK-1 levels, through the Wnt/β-catenin signaling pathway
216 and yet another so far unknown mechanism.
217 In a search for a SKMc15-specific regulatory mechanism of Dlk-1 levels we focused on the translational
218 regulation since previously was shown that general reduction of protein synthesis and downregulation of the
219 expression and translational efficiency of ribosomal proteins are events crucial for the regulation of adipocyte
220 differentiation [17]. Interestingly, IFRD2 (SKMc15) was recently identified as a novel specific factor capable of
221 translationally inactivating ribosomes [16]. Because SKMc15 may play a crucial role in the adipogenesis
222 regulation we tested in our following experiment the effect of SKMc15 knockout on the general translational
223 efficiency of WT, TIS7, SKMc15 single and double KO MEFs. Cells were incubated 30 minutes in the absence

224 of methionine and cysteine, followed by one hour in the presence of ^{35}S-methionine. As shown in Figure 5a,
225 there was a significant increase in the general translational activity of MEFs lacking SKMc15 alone or both
226 TIS7 and SKMc15, but not in TIS7 single knockout cells. Therefore, we concluded that SKMc15 alone, but
227 not TIS7 inhibits the general translational activity necessary for the induction of adipogenic differentiation,
228 also via the translational regulation of Dlk-1. This finding supported the result shown in Figure 3d where the
229 DLK-1 protein levels were significantly induced in WAT samples isolated from SKMc15 single knockout mice.
230

231 *TIS7 and SKMc15 regulate adipocyte differentiation through DLK-1, MEK/ERK pathway, PPARγ and*
232 *C/EBPα.*

233 DLK-1 protein carries a protease cleavage site in its extracellular domain [38] and is secreted. The extracellular
234 domain of DLK-1 is cleaved by ADAM17, TNF-α Converting Enzyme to generate the biologically active
235 soluble DLK-1 [19]. DLK-1 mRNA and protein levels are high in preadipocytes but DLK-1 expression is absent
236 in mature adipocytes. Hence, adding soluble DLK-1 to the medium inhibits adipogenesis [39]. To test if the dKO
237 MEFs secreted DLK-1, cell culture media from MEFs treated 8 days with the adipocyte differentiation cocktail
238 were collected and analyzed by Western blotting. As shown in Figure 5b, dKO cells secreted DLK-1 protein,
239 but in an identical volume of the cell culture medium from WT MEFs no DLK-1 could be detected. To prove
240 that secreted DLK-1 could inhibit adipocyte differentiation of dKO MEFs, we cultured WT MEFs with
241 conditioned medium from dKO MEFs. Adipocyte differentiation of WT MEFs was strongly inhibited by the
242 dKO MEFs-conditioned medium when compared to the control WT cells (Figure 5c, quantified in Figure 5d).
243 Based on these results we concluded that cells derived from dKO mice express increased DLK-1 levels and
244 secreted, soluble DLK-1 may inhibit adipocyte differentiation *in vivo*.

245 Previous studies showed that soluble DLK-1 activates MEK/ERK signaling, which is required for inhibition of
246 adipogenesis [20]. As DLK-1 was strongly up regulated in dKO MEFs during adipocyte differentiation we
247 subsequently analyzed possible activation of the MEK/ERK pathway (Figure 6a). The phosphorylation of p44
248 and of p42 was up regulated 5-fold and 3-fold ($P<0.05$), respectively, in the adipocyte-differentiated dKO

249 when compared to the WT MEFs (Figure 6b). Previously, activation of MEK/ERK by DLK-1 was shown to up
250 regulate the expression of the transcription factor SOX9, resulting in the inhibition of adipogenesis [33].
251 Therefore, we measured SOX9 mRNA expression by RT qPCR in 8 days adipocyte-differentiated MEFs.
252 SOX9 expression was significantly (P<0.001) up regulated in 8 days adipocyte-differentiated dKO when
253 compared to WT MEFs (Figure 6c).
254 The adipocyte differentiation deficiency of dKO MEFs suggested that C/EBPα and PPARγ might also be
255 regulated through TIS7 and/or SKMc15. It was previously shown that elevated levels of the cleaved
256 ectodomain of DLK1 have been correlated with reduced expression of PPARγ [40]. Therefore, we analyzed the
257 differences in PPARγ expression between WT and dKO MEFs during their differentiation into adipocytes.
258 While PPARγ expression was strongly induced during adipocyte differentiation from WT MEFs this was
259 barely detectable in dKO MEFs (Figure 7a) and also C/EBPα expression was never induced up to the levels
260 of WT (Figure 7b). In a rescue experiment we showed that the co-expression of TIS7 and SKMc15 in
261 undifferentiated MEFs strongly increased the expression of the PPARγ in dKO MEFs (P<0.001), almost up
262 to the levels of WT MEFs (Figure 7c). The expression of C/EBPα was also strongly up regulated by the co-
263 expression of TIS7 and SKMc15 (P<0.01) (Figure 7d). Based on these results we concluded that TIS7 and
264 SKMc15 regulate the expression of both PPARγ and C/EBPα, both crucial for adipocyte differentiation.
265
266 *TIS7 and SKMc15 regulate the expression of the lipid transporters CD36 and DGAT1.*
267 PPARγ induces the expression of CD36, a very long chain fatty acids (VLCFA) transporter in heart, skeletal
268 muscle, and also adipose tissues [41]. The regulation of CD36 by PPARγ contributes to the control of blood
269 lipids. Interestingly, CD36 null mice exhibit elevated circulating LCFA and triglycerides levels consistent with
270 the phenotype of dKO mice and CD36 deficiency partially protected from HFD-induced insulin resistance [42].
271 Because of down regulated PPARγ levels in adipose tissues of dKO mice we decided to study in more detail
272 the regulation of CD36 in these as well. We have found strongly reduced CD36 mRNA expression levels in
273 WAT from dKO mice (64 % of the WT values) (Figure 8a). Next, we analyzed CD36 in WT and dKO MEFs

274 before onset and during adipocyte differentiation. As long as CD36 mRNA expression substantially increased
275 in WT MEFs, there were almost undetectable transcript levels of CD36 in dKO cells treated with the adipocyte
276 differentiation cocktail (Figure 8b). Diacylglycerol acyltransferase 1 (DGAT1), a protein associated with the
277 enterocytic triglyceride absorption and intracellular lipid processing [83] is besides CD36 another target gene
278 of adipogenesis master regulator PPARγ [43]. DGAT1 mRNA levels are strongly up regulated during adipocyte
279 differentiation [44], its promoter region contains a PPARγ binding site [45] and DGAT1 is also negatively regulated
280 by the MEK/ERK pathway [46] . DGAT1 expression was shown to be increased in TIS7 transgenic mice [3] and
281 its expression was decreased in the gut of high fat diet-fed TIS7 KO mice [8]. Importantly, DGAT1 expression
282 in adipocytes and WAT is up regulated by PPARγ activation [43]. Therefore, we measured DGAT1mRNA levels
283 during the differentiation of WT and dKO MEFs into adipocytes to analyze the role of TIS7 and SKMc15 on
284 the regulation of this protein involved in adipogenesis and triglyceride processing. As long as DGAT1
285 expression substantially increased during the differentiation of WT MEFs, there was no difference in DGAT1
286 mRNA levels in dKO cells treated with the adipocyte differentiation cocktail (Figure 8c). Therefore, we
287 concluded that both, TIS7 and SKMc15 regulate expression of multiple proteins involved in adipocyte
288 differentiation and function, thereby contributing to the lean phenotype of dKO mice.
289

290 **Discussion**

291 In this study we show that simultaneous depletion of TIS7 and of its orthologue SKMc15, a protein recently
292 identified as a translational inhibitor, caused severe reduction of adipose tissues and resistance against high
293 fat-induced obesity in mice. We identified two parallel mechanisms leading to a deficiency in adipocyte
294 differentiation. Firstly, TIS7-regulated Wnt signaling affected Dlk-1 transcription and secondly, our study
295 provided the first experimental evidence for SKMc15 acting as a translational inhibitor that among other
296 proteins might control DLK-1 protein levels, thereby also contributing to the regulation of adipogenesis (Figure
297 9).

298 dKO mice were phenotypically similar with both, CD36 deficient and DLK-1 transgenic mice, namely in
299 decreased amounts of WAT and resistance to HFD-induced obesity. Previous studies showed that over-
300 expression of TIS7 caused increased intestinal lipid transport resulting in elevated body weight gain during
301 HFD feeding [36]. Knockout of TIS7 and SKMc15 impaired absorption of free fatty acids from the lumen into
302 enterocytes and reduced rate of fat absorption from intestines into the circulation. Simultaneously, higher
303 concentrations of free fatty acids in the feces of dKO mice suggested that mice lacking TIS7 and SKMc15
304 suffer from an intestinal lipid uptake deficiency, yet another contributing reason for the lean phenotype of
305 these mice (data not shown). In dKO mice we found inhibited PPARγ and C/EBPα levels, induced MEK/ERK
306 pathway, and decreased expression of CD36 and DGAT1, all hallmarks of up regulated DLK-1, a known
307 adipogenesis inhibitor. TIS7 and SKMc15 acted after the commitment to the preadipocyte stage since the
308 elevated DLK-1 and β-catenin levels found in WAT of dKO mice were characteristic for the preadipocyte
309 stage [47].
310 It is known that disruption of Wnt signaling in embryonic fibroblasts results in spontaneous adipocyte
311 differentiation [48] and opposite, stabilized β-catenin keeps cells in the preadipocyte stage [23]. Consistent with
312 this knowledge we found up regulated β-catenin protein levels in WAT of dKO mice and increased Wnt
313 signaling activity in dKO MEFs. It has to be mentioned that our data were different to those by Nakamura *et*
314 *al.* who showed that following the TIS7 overexpression in adipocytes was up regulated Wnt/β-catenin
315 signaling and inhibited oil red O staining [5]. However, one has to take into consideration the difference in cell
316 systems used in these two studies. All results presented in Nakamura's study were obtained in 3T3-L1 cells
317 fibroblasts following overexpression of TIS7. Opposite to that, we have studied the role of endogenous TIS7
318 in cells derived from wild type or knockout mice. Moreover, we have found ubiquitous TIS7 expression in all
319 WT mouse organs without any pre-treatment such as e.g. hypoxia. On the other hand, Nakamura *et al*.
320 identified up regulated TIS7 expression levels in WAT of obesity model mice. This result, however, fully
321 supports our findings of lean phenotype in TIS7 and SKMc15 dKO mice.

322 We demonstrated that in dKO MEFs, induced for adipocyte differentiation, the increase in Wnt signaling led
323 to up regulated binding of β-catenin to the DLK-1 gene regulatory elements, resulting in sustained DLK-1
324 expression. In adipogenesis DLK-1 expression is down regulated through histone methylation by COPR5
325 and PRMT5 that prevent β-catenin binding to the DLK-1 gene [31]. Interestingly, in dKO MEFs we found weaker
326 binding of dimethylated H4R3 to the DLK-1 gene that was consistent with our previous findings on the
327 negative role of TIS7 in epigenetic regulation of gene expression including the PRMT5 activity [14].
328 There was a difference in effects of ectopic expression of TIS7, SKMc15 and their co-expression on DLK-1
329 levels (data not shown), confirming the hypothesis TIS7 and SKMc15 regulate DLK-1 levels via two
330 independent pathways/mechanisms. Despite the fact that SKMc15 knockout had no effect on Wnt signaling
331 it nevertheless affected DLK-1 levels, suggesting a contribution of SKMc15 to its regulation. Since SKMc15
332 was identified as a novel factor translationally inactivating ribosomes [16] and since down regulation of the
333 protein synthesis machinery is an essential regulatory event during early adipogenic differentiation [17], we
334 hypothesize that SKMc15 regulates DLK-1 levels through translational regulation, however additional
335 investigations will be necessary to confirm this mechanism. Elevated DLK-1 levels in dKO MEFs activated
336 the MEK/ERK pathway thereby decreasing PPARγ and C/EBPα levels important for adipogenic
337 differentiation. Besides that, the expression of SOX9 was up regulated, suggesting that the dKO MEFs keep
338 their proliferative state and cannot enter differentiation into mature adipocytes [20].
339 Down regulation of PPARγ and C/EBPα implied changes in expression of downstream adipogenesis-related
340 genes. Among them, decreased CD36 and DGAT1 levels were a plausible explanation of the dKO mice lean
341 phenotype since it is known that both proteins play a functional role in differentiation of murine adipocytes
342 and their deficiency impairs fat pad formation independent of lipid uptake [49]. Our findings implicate that TIS7
343 and SKMc15 play a up to now unknown role in the regulation of CD36 and therefore possibly contribute to
344 CD36 related pathogenesis of human metabolic diseases, such as hypoglycemia [50], hypertriglyceridemia [51],
345 and disordered fatty acid metabolism [52, 53].

346 We and others have previously shown that TIS7 is involved under both, chow and HFD conditions in intestinal
347 triglyceride absorption. Here we show for the first time the role of TIS7 and its orthologue SKMc15 in
348 adipocyte differentiation. Moreover, our data presented here document the physiological function of SKMc15
349 as a translational inhibitor. To our surprise, although TIS7 and SKMc15 share high sequence homology and
350 a functional role in the adipogenesis, they use two independent regulatory mechanisms.
351

352 **Methods**

353 *Generation of animal models.* All animal experiments were performed in accordance with Austrian legislation
354 BGB1 Nr. 501/1988 i.d.F. 162/2005).
355 Mice lacking TIS7 were previously described [4]. SKMc15 KO mice generation: targeting construct contained
356 SKMc15 gene locus exons. A loxP site and a neomycin resistance gene inserted at position 105515
357 (AY162905). The neomycin cassette was flanked by two frt sites. A second loxP site was inserted at position
358 102082 (AY162905). Further downstream, 15 additional nucleotides, part of intron 1, exon 2 (splice site:
359 donor and acceptor) and the CDS of hrGFP from the Vitality hrGFP mammalian expression vector pIRES-
360 hrGFP-2a (Stratagene) were added. The targeted construct was electroporated into Sv129 mouse ES cells.
361 After the selection with G418 single cell clones were screened by PCR and confirmed by Southern blot
362 analysis. After Cre recombinase treatment cell clones were screened by PCR. Clones with floxed gene
363 deleted, were used for blastocyst injection into C57Bl/6J mice. Two male chimeras with ≥ 40 % or more
364 agouti coat color were mated to C57Bl6 females. The knockout mouse strain was derived from one male
365 mouse carrying the allele of interest. Heterozygous mice were back-crossed to C57Bl6 mice for 9
366 generations. dKO mice were generated by crossing the SKMc15 KO mice with the TIS7 single KO mice. The
367 resulting mice were screened by PCR and double heterozygous mice used for further breeding until
368 homozygosity. In order to achieve maximal homogeneity of experimental groups, in all experiments
369 presented here we used only male mice.
370

371 *SKMc15 knockout Southern blot analysis*. XbaI restriction sites (position 109042; position 102079; position
372 92253) located in the SKMc15 locus (AY162905). Fragment detected by the Southern probe: 9.6 kb wt
373 (Supplementary figure 3a, insert, band V); 15 kb in deleted locus (band IV). The 566 bp long probe for
374 hybridization from genomic DNA (96605 – 97171; AY162905). PCR primer sequences: RK 150 Fwd: 5'-
375 GGTCCTGCCACTAATGCACTG-3'; RK 151 Rev: 5'- GCAGACAGATGCCAGGAAGAC-3'.
376
377 *SKMc15 knockout PCR genotyping analysis*. hrGFP insert in the 3´ UTR detected by primer GFP2 5´-
378 AGCCATACCACATTTGTAGAG-3´ and RK101 3´ UTR (5´-TGATGATAGCTTCAAAGAGAA-3´; 100617 –
379 100591 of the SKMc15 locus (AY162905). PCR product 1700 bp. SKMc15 detection: RG1; 5´-
380 TGTGGCCTTTATCCTGAGTC-3´; 102286–102266) and RG2; 5´-TGGCTTCATTTACACTACTCCTT-3´;
381 101860 – 101882 primers (Supplementary figure 3a). WT allele PCR product 426 bp and the targeted allele
382 PCR product 1772 bp (Supplementary figure 3b). TIS7 genotype tested as explained previously [4]
383 (Supplementary figure 3c).
384
385 *Growth monitoring and body composition measurement*. Mice weaned at 3 weeks, regular chow diet,
386 weighed weekly. Dual energy X-ray absorptiometry was measured with Norland scanner (Fisher Biomedical).
387 Micro-CT experiments performed using vivaCT 40 (Scanco Medical AG). The scans were performed using
388 250 projections with 1024 samples, resulting in a 38µm isotropic resolution. Tube settings: 45kV voltage,
389 177µA current, integration time 300ms per projection. Image matrix 1024*1024 voxels and a grayscale depth
390 of 16 bit. The length of the image stack was individually dependent, starting from the cranial end of the fist
391 lumbar vertebrae, to the caudal end of the fifth lumbar vertebrae. The image reconstruction and post
392 processing were performed using the Scanco Medical system software V6.6. For the adipose tissue
393 evaluation an IPL (image processing language) script by Judex et al., provided by Scanco medical AG was
394 modified to the scanner individual parameters leading to 2 values lower threshold than in the original script
395 for the adipose tissue filters 76. The script calculated the total abdominal volume without potential air in the

396 cavities. A separation of subcutaneous and visceral fat mass was used only for visualization. For the
397 quantitative fat mass analysis we used 56 male 5 to 12 month old mice (mean age 9.35 ± 2.03 month)
398 reflecting an adult to mid aged cohort defined by Flurkey et al. 2007 [54]. The development of adipose tissue
399 in healthy mice is stable between 4 and 12 months [55]. Therefore, sex and age could have only very limited
400 influence on the experimental results. For the quantitative comparison, the percent contribution of the
401 abdominal fat to the body weight was calculated using a mean weight of 0.9196 g/ml for adipose tissue [54].
402 Statistics were performed using an ANCOVA with a Bonferroni corrected Post Hoc testing on the µCT fat
403 data and the body mass data.
404
405 *Metabolic measurements*. The indirect calorimetry trial monitoring gas exchange, activity, and food intake
406 was conducted over 21 hours (PhenoMaster TSE Systems). Body mass and rectal body temperature before
407 and after the trial were measured. The genotype effects were statistically analyzed using 1-way ANOVA.
408 Food intake and energy expenditure were analyzed using a linear model including body mass as a co-variate.
409
410 *HFD feeding*. Age-matched (7-week-old) male TIS7-/- SKMc15-/- and WT mice were caged individually and
411 maintained up to 3 weeks on a synthetic, high saturated fat (HFD) diet (TD.88137; Ssniff). Animals were
412 weighted every 4th day between 08:00 and 10:00. Small intestines were harvested for oil red O staining to
413 detect lipid accumulation. Intestines, liver, muscles and adipose tissue were collected for total RNA and
414 protein isolation. Unfixed intestines were flushed with PBS using a syringe, embedded in Tissue-Tek (Sakura,
415 4583) and frozen in liquid nitrogen for immunohistochemical analysis.
416
417 *Quantitative food consumption and fecal fat determination.* Adult mice were acclimatized to individual caging
418 and to the HFD for a week, monitored for weight gain and their food intake daily. The daily food intake data
419 were pooled for the following 7 days and the food intake was estimated (g/day). Feces were collected daily
420 and weighted for 7 days after second week of the HFD consumption.

421

422 *Antibodies, viral and cDNA constructs*. Antibodies: anti-CD36 AbD Serotec (MCA2748), Abcam (ab36977),
423 p44/42 MAPK (Erk1/2) and Phospho-p44/42 MAPK (Erk1/2) (Thr202/Tyr204) Cell Signaling Technology
424 (9102, 9101), β-catenin antibody Sigma (C2206), anti-DLK Abcam (ab119930), anti-histone H4R3me2s
425 antibody Active Motif (61187). For ChIP experiments were used anti-TIS7 [11] and anti-SKMc15 [4] rabbit
426 polyclonal antibodies previously proven for ChIP suitability in [14]. pTOPflash reporter construct was a gift from
427 H. Clevers (University of Utrecht, Holland). TIS7 construct was described previously [11]. Partial cds of
428 mSKMc15 was amplified by PCR and cloned into pcDNA3.1(-)/MycHis6 (Invitrogen).

429

430 *Cell culture and adipocyte differentiation*. MEFs were generated from 16-day old embryos. After dissection
431 of head for genotyping, removal of limbs, liver and visceral organs embryos were minced and incubated in 1
432 mg/mL collagenase (Sigma-Aldrich, C2674) 30 mins at 37°C. Embryonic fibroblasts were maintained in
433 growth medium containing DMEM high glucose (4.5 g/l); sodium pyruvate, L-glutamine, 10% FCS (Invitrogen,
434 41966029), 10% penicillin/streptomycin at 37°C in 5% CO_2. Adipocyte differentiation treatment was medium
435 with 0.5 mM 3-isobutyl-1-methylxanthine (I5879), 1 µM dexamethasone (D4902), 5 µg/ml insulin (I2643) and
436 1 µM Rosiglitazone (Sigma-Aldrich, R2408). After 3 days growth medium containing 1 µg/ml insulin cells
437 were differentiated for 8 days. To visualize lipid accumulation adipocytes were washed with PBS, fixed with
438 6 % formaldehyde overnight, incubated with 60 % isopropanol, air dried and then incubated with oil red O.
439 Microscopic analysis was followed by isopropanol elution and absorbance measurement at 490 nm.

440

441 *Analysis of translation by metabolic labelling.* Pulse labelling of mitochondrial proteins was performed as
442 described before [56], with the following changes: 1x 10^6 wild-type and dKO MEFs cells per plate were seeded
443 and cultivated for 24 h. Cells were washed twice with PBS followed by one wash with labelling medium (ESC
444 medium without cysteine and methionine) and a 30 min incubation in labelling medium. To label newly
445 translated products, 200 µCi of [^{35}S]-methionine (10 mCi/ml; Hartman Analytic) were added and the cells

446 were incubated for 1 h. Cells were washed and incubated another 10 min in standard medium at 37 °C. Cells
447 were then harvested by trypsinizing, washed once with ice-cold PBS, extracted with ice-cold RIPA buffer
448 containing protease-inhibitors and briefly sonicated. Proteins were fractionated by gel electrophoresis in 16%
449 Tricine gels (Invitrogen) and stained with Coomassie brilliant blue, and radioactive signals were visualized
450 by phosphorimaging. Signal intensities were quantified using the Image Studio Lite (v5.2) software.
451
452 *RT-PCR*. Tissues from animals fed for 3 weeks with HFD were snap frozen and stored at –80°C. Total RNA
453 was isolated using the TRIzol reagent (Invitrogen, 15596026). RNA was then chloroform-extracted and
454 precipitated with isopropanol. The yield and purity of RNA was determined by spectroscopic analysis; RNA
455 was stored at –80°C until use.
456
457 *Quantitative RT-PCR and statistics*. Total RNA were treated with DNAse1 and reverse transcribed to cDNA
458 by Revert Aid First Strand cDNA Synthesis Kit (Thermo Scientific, K1622) with oligo dT primers. Quantitative
459 RT-PCR was performed using Taqman probes and primer sets (Applied Biosystems) specific for CD36
460 (assay ID Mm00432398_m1), Dgat1 (Mm00515643_m1), Pparγ (Mm00440940_m1), C/EBPα
461 (Mm00514283_s1), DLK-1 (Mm00494477_m1) and Sox9 (Mm00448840_m1). Ribosomal protein 20 (assay
462 ID Mm02342828_g1) was used as normalization control for quantification by the ddCt method. PCR reactions
463 were performed using 10 µl cDNA in PikoReal 96 real-time PCR system (Thermo Scientific). Quantification
464 data were analyzed by 2-tailed, type 2 Student's t test.
465
466 *Transient transfections and luciferase assay*. pGL2-Basic (Promega, E1641) or pGLCD36 [57] were used as
467 reporter constructs. Expression constructs or empty vector DNA as a control were co-transfected. pCMV-β-
468 Gal plasmid was used to normalize for transfection efficiency. For luciferase reporter assays, 1.5x105 cells
469 were seeded into 24-well plates and transfected after 24 hours with indicated plasmid combinations using
470 Lipofectamine Plus™ Reagent (Invitrogen, 15338030). The total amount of transfected DNA (2 µg DNA per

471 well) was equalized by addition of empty vector DNA. Cells were harvested 48 h post-transfection in 0.25 M
472 Tris, pH 7.5, 1% Triton X-100 buffer and assayed for both luciferase and β-galactosidase activities. Luciferase
473 activity and β-galactosidase activity were assayed in parallel by using the Lucy 2® detection system (Anthos).
474 Transfections were performed in triplicates and all experiments were repeated several times.
475
476 *Chromatin immunoprecipitation (ChIP)*. Chromatin was isolated from TIS7 WT and dKO formaldehyde-
477 treated, 8 days adipocyte differentiated MEFs using the EpiSeeker Chromatin Extraction Kit (Abcam,
478 ab117152). ChIP analyses were carried out as described previously [58]. Sequence of the oligonucleotides for
479 two regions of the Dlk-1 promoter, encompassing TCF and β-catenin binding sites were as defined in [31].
480 Sonicated chromatin was centrifuged at 15.000x g for 10 min at 4°C, and the supernatant (65 µg of sheared
481 DNA per each IP) was diluted ten-fold with cold ChIP dilution buffer containing 16.7 mM Tris-HCl pH 8.1, 167
482 mM NaCl, 0.01% (w/v) SDS, 1.1% (w/v) Triton X-100 and 1.2 mM EDTA with protease inhibitors. Samples
483 were pre-cleared for 1 h with protein A Sepharose CL-4B (Sigma-Aldrich, 17-0780-01) beads blocked with
484 0.2 µg/µl sonicated herring sperm DNA (Thermo Fisher, 15634017) and 0.5 µg/µl BSA (NEB, B9000 S).
485 Immunoprecipitations were performed at 4°C overnight. Immune complexes were collected with protein A
486 Sepharose for 1h at 4°C followed by centrifugation at 1000 rpm and 4°C for 5 min. Beads were washed with
487 1ml low salt wash buffer (20 mM Tris-HCl pH 8.1, 150 mM NaCl, 0.1%(w/v) SDS, 1%(w/v) Triton X-100
488 (Merck), 2 mM EDTA), high salt wash buffer (20 mM Tris-HCl pH 8.1, 500 mM NaCl, 0.1% (w/v) SDS, 1%
489 (w/v) Triton X-100, 2 mM EDTA), LiCl wash buffer (10 mM Tris-HCl pH 8.1, 250 mM LiCl, 1% (w/v) sodium
490 deoxycholate, 1% (w/v) IGEPAL-CA630, 1 mM EDTA) for 5 min at 4°C on a rotating wheel, and twice with 1
491 ml TE buffer (10 mM Tris-HCl pH 8.0, 1 mM EDTA). Protein-DNA complexes were eluted from antibodies by
492 adding a freshly prepared elution buffer containing 1% SDS and 0.1 M $NaHCO_3$. The eluate was reverse
493 cross linked by adding NaCl to a final concentration of 0.2 M and incubating at 65 °C for four hours.
494 Afterwards the eluate was treated with Proteinase K at 45 °C for 1 hour. The immunoprecipitated DNA was
495 then isolated by phenol/chloroform precipitation and used as a template for real-time-quantitative PCR. The

496 primer pairs specific for regulatory regions of the Dlk-1 gene were selected as described before [31]. Reactions
497 with rabbit IgG or with 1.23% of total chromatin (input) were used as controls. For real-time-quantitative PCR
498 a PikoReal System was used. Signals were normalized to input chromatin and shown as % input. The raw
499 cycle threshold (Ct) values of the input were adjusted to 100% by calculating raw Ct – log2(100/input). To
500 calculate the % input of the immunoprecipitations, the equation 100 × 2[Ct (adjusted input to 100%) – Ct (IP)]
501 was applied.
502
503 *Statistics*. Unpaired, 2-tailed Student's t tests were used for all statistical comparisons. A P value of < 0.05
504 was considered significant.
505

506 **Acknowledgements**

507 The authors thank Robert Kurzbauer for generation of dKO mice, Stephan Geley, Laura M. de Smalen and
508 Karin Schluifer for the technical assistance, David Teis and Zlatko Trajanoski for critical reading of the
509 manuscript. Furthermore, the Animal Facility of Medical University Innsbruck for their care of our mice. This
510 work was supported by P18531-B12 and P22350-B12 grants from the Austrian FWF grant agency to Ilja
511 Vietor and by the German Federal Ministry of Education and Research (Infrafrontier grant 01KX1012) to
512 Martin Hrabe de Angelis.
513

514 **Author contributions**

515 I.V., D.C., M.D.E., V.K., J.Ro., M.K., T.V. and L.A.H. designed the study. I.V., D.C., K.P., R.G., J.Ro., M.H.,
516 V.K., G.D., F.S., and T.V. performed experiments. I.V., D.C., T.V. and L.A.H. wrote the manuscript.
517

518 **Figure legends**

519 **Figure 1. dKO mice display postnatal growth retardation and less body fat.**

520 a) Growth curves of WT and dKO mice on chow diet (n fluctuate depending on the time point of
521 measurement). b) DEXA measurements of WT and dKO mice. Left panel depicts the absolute values of fat
522 and lean mass per animal and the right panel represents values normalized to the total body weight of
523 animals (n=15). c) Micro-computed tomography measurements identified a lack of abdominal fat in single
524 and dKO mice. 3-dimensional reconstitution of images of the abdominal fat mass distribution in WT and KO
525 mice. Yellow color represents subcutaneous and red visceral fat mass. Black compartments are shadows
526 resulting as part of the lightning model for the 3D volume rendering.
527
528 **Figure 2. dKO mice are resistant against HFD-induced obesity.**
529 a) Mass contribution [%] of the abdominal fat in correlation to the total body weight [g]. A linear regression
530 is overlaid for each group individually. The regression results for the WT group are y= 0,342x-11,13 with a
531 R^2 of 0,74; for the TIS7 KO group y=0,143x-3,91 with a R^2 of 0,82; for the SKMc15 KO y=0,005x+0,48 with
532 a R^2 of 0,04 and for the dKO y=0,011+0,01 with a R^2 of 0,1. ANCOVA analysis for the fat mass as a
533 percentage of the body weigth as covariant was performed. b) Effect of single SKMc15 or TIS7 knockout
534 and TIS7 SKMc15 double knockout on total body weight in [g] and body fat amount normalized to the body
535 weight in [%]. c) TIS7 and SKMc15 knockout reduced the gain of body weight of mice fed with HFD. 7
536 weeks old male WT and dKO mice were caged individually and maintained up to 21 days on HFD. Data
537 shown are mean ± SEM, n≥9 per genotype, *P< 0.05, **P < 0.01, *** P < 0.001.
538
539 **Figure 3. Adipocyte differentiation and Wnt signaling pathway are significantly affected in dKO**
540 **mice.** a) Representative oil red O staining of MEF cells following 8 days of the adipocyte differentiation
541 protocol. Images were cropped and space bars represents always 20µm. b) Quantification of oil red O
542 staining from three independent adipocyte differentiation experiments. Student's t-test ***P<0.001. c) Wnt
543 signaling activity was measured in MEFs transiently co-transfected with the Tcf reporter plasmid pTOPflash
544 and β-galactosidase expression vectors. Transfection efficiency was normalized using the β-galactosidase

545 values. The experiment was repeated three times. Data shown are mean ± SEM. d) Top panel: Western
546 blot analysis of β-catenin amounts in WAT samples. One representative Western blot from 3 biological
547 repetitions is shown. Bottom panel: DLK-1 is significantly up regulated both in TIS7, SKMc15 single KO and
548 also in dKO mice.
549
550 **Figure 4. DLK-1 levels are lower and β-catenin binding to the Dlk-1 gene is increased in dKO MEFs.**
551 a) DLK-1 mRNA expression measured by qPCR in WAT and MEFs. Values were normalized on GAPDH,
552 n=3. Error bars indicate standard deviations. b) DLK-1 mRNA expression measured in MEFs treated with
553 the adipocyte differentiation cocktail for given times. WT MEFs values were set as 1. c) DLK-1 protein
554 Western blot analysis in MEFs after 8 days of adipocyte differentiation. Mean of 3 biological repeats; insert
555 is one representative Western blot. d) DLK-1 mRNA levels in dKO MEFs were down regulated following
556 ectopic co-expression of TIS7 and SKMc15. mRNA expression levels were analyzed by RT qPCR 48 hours
557 following the transfection. WT MEFs values were set as 1, n=3; Student's t-test *P<0.05. Error bars indicate
558 standard deviations. e) Recruitment of indicated proteins to regulatory regions of the Dlk-1 promoter in WT
559 and KO MEFs was analyzed by ChIP at day 8 of the adipocyte differentiation. Values are expressed as the
560 percentage of immunoprecipitated chromatin relative to input and are the mean of triplicates. ChIP analysis
561 identified increased specific β-catenin binding to its DLK-1 regulatory element in dKO samples. Pre-immune
562 serum and IgG were used as background controls. n=3, Data shown are mean ± SEM, Student's t-test ***P
563 < 0.001.
564
565 **Figure 5. SKMc15 is a translational inhibitor. Up regulated DLK-1 in dKO MEFs inhibits adipocyte**
566 **differentiation.** a) translational analysis – *in vivo* metabolic staining of MEFs with ^{35}S-methionine. Equal
567 numbers of cells were seeded and 24 hours later treated as explained in Methods section. Identical volumes
568 of cell lysates were separated by SDS-PAGE, gel was dried and analyzed by a phosphorimager. Equal
569 loading was documented by the Coomassie blue staining of the gel. b) dKO MEFs secrete DLK-1 protein into

570 the cell culture medium. Identical volumes of media from WT and dKO cells 8 days treated with the adipocyte
571 differentiation cocktail were analyzed by Western blot. Equal loading of samples was evaluated by amido
572 black staining of the membrane. c) dKO MEFs-conditioned medium inhibited adipocyte differentiation in WT
573 MEFs. MEFs were treated 8 days with the adipocyte differentiation cocktail. WT MEFs treated with the dKO-
574 conditioned medium showed reduced differentiation. Images were cropped and space bars represent always
575 20µm. d) Quantification of the oil red O staining of samples shown in panel C.
576
577 **Figure 6. MAPK signaling and Sox9 expression are induced in dKO MEFs.**
578 a) Representative Western blots of phospho-p44 and phospho-p42 from 8 days adipocyte differentiation
579 cocktail-treated MEFs. b) Normalization on p44 and p42; n=3. Error bars indicate standard deviations. WT
580 values were set as 100 %. c) SOX9 mRNA levels were up regulated in dKO MEFs. SOX9 expression was
581 measured by qPCR in 8 days adipocyte-differentiated WT and dKO MEFs. SOX9 values were normalized
582 on GADPH expression. WT MEFs values were set as 1, n=3. Data shown are mean ± SEM. Student's t-test
583 **P < 0.01.
584
585 **Figure 7. Adipocyte differentiation regulatory genes are down regulated in dKO mice.**
586 a) PPARγ and b) C/EBPα mRNA levels were down regulated in dKO adipocyte-differentiated MEFs. Gene
587 expression was measured by qPCR during the treatment with the adipocyte differentiation cocktail. Values
588 were normalized on GADPH expression. WT MEFs values were set as 1, n=3. Data shown are mean ±
589 SEM. c) Ectopic co-expression of TIS7 and SKMc15 in undifferentiated MEFs significantly increased levels
590 of adipogenic genes PPARγ and d) C/EBPα. Student's t-test **P < 0.01, ***P < 0.001.
591
592 **Figure 8. Target genes of adipocyte differentiation regulatory genes are down regulated in dKO mice.**
593 a) qPCR analysis of CD36 mRNA levels in WAT, *P< 0.05 b) qPCR analysis of CD36 in MEFs
594 differentiating into adipocytes. Relative expression levels were normalized on GAPDH expression. WT

595 MEFs values were set as 1. c) DGAT1 mRNA levels were down regulated in dKO adipocyte-differentiated
596 MEFs, ***P < 0.001.
597
598 **Figure 9. Proposed model of TIS7 and SKMc15 molecular mechanisms of action during adipocyte**
599 **differentiation.**
600 Two parallel mechanisms leading to a deficiency in adipocyte differentiation: TIS7-regulated Wnt signaling
601 affected Dlk-1 transcription and SKMc15 acting as a translational inhibitor also contributed to the regulation
602 of adipogenesis.
603
604 **Conflict of interest.**
605 The authors declare that they have no conflict of interest.
606
607 **References**
608
609 1. Sarantopoulos CN, Banyard DA, Ziegler ME, Sun B, Shaterian A, Widgerow AD. Elucidating the
610 Preadipocyte and Its Role in Adipocyte Formation: a Comprehensive Review. *Stem Cell Rev* 2018,
611 **14**(1)**:** 27-42.
612
613 2. Iacopetti P, Barsacchi G, Tirone F, Cremisi F. Expression of the PC4 gene in the developing rat
614 nervous system. *Brain Res* 1996, **707**(2)**:** 293-297.
615
616 3. Wang Y, Iordanov H, Swietlicki EA, Wang L, Fritsch C, Coleman T*, et al.* Targeted intestinal
617 overexpression of the immediate early gene tis7 in transgenic mice increases triglyceride
618 absorption and adiposity. *J Biol Chem* 2005, **280**(41)**:** 34764-34775.
619
620 4. Vadivelu SK, Kurzbauer R, Dieplinger B, Zweyer M, Schafer R, Wernig A*, et al.* Muscle
621 regeneration and myogenic differentiation defects in mice lacking TIS7. *Mol Cell Biol* 2004,
622 **24**(8)**:** 3514-3525.
623
624 5. Nakamura Y, Hinoi E, Iezaki T, Takada S, Hashizume S, Takahata Y*, et al.* Repression of
625 adipogenesis through promotion of Wnt/beta-catenin signaling by TIS7 up-regulated in
626 adipocytes under hypoxia. *Biochim Biophys Acta* 2013, **1832**(8)**:** 1117-1128.
627
628 6. Vietor I, Kurzbauer R, Brosch G, Huber LA. TIS7 regulation of the beta-catenin/Tcf-4 target gene
629 osteopontin (OPN) is histone deacetylase-dependent. *J Biol Chem* 2005, **280**(48)**:** 39795-39801.

630
631 7. Iezaki T, Onishi Y, Ozaki K, Fukasawa K, Takahata Y, Nakamura Y*, et al.* The Transcriptional
632 Modulator Interferon-Related Developmental Regulator 1 in Osteoblasts Suppresses Bone
633 Formation and Promotes Bone Resorption. *J Bone Miner Res* 2016, **31**(3)**:** 573-584.

634
635 8. Yu C, Jiang S, Lu J, Coughlin CC, Wang Y, Swietlicki EA*, et al.* Deletion of Tis7 protects mice from
636 high-fat diet-induced weight gain and blunts the intestinal adaptive response postresection. *J*
637 *Nutr* 2010, **140**(11)**:** 1907-1914.

638
639 9. Garcia AM, Wakeman D, Lu J, Rowley C, Geisman T, Butler C*, et al.* Tis7 deletion reduces survival
640 and induces intestinal anastomotic inflammation and obstruction in high-fat diet-fed mice with
641 short bowel syndrome. *Am J Physiol Gastrointest Liver Physiol* 2014, **307**(6)**:** G642-654.

642
643 10. Micheli L, Leonardi L, Conti F, Buanne P, Canu N, Caruso M*, et al.* PC4 Coactivates MyoD by
644 Relieving the Histone Deacetylase 4-Mediated Inhibition of Myocyte Enhancer Factor 2C. *Mol*
645 *Cell Biol* 2005, **25**(6)**:** 2242-2259.

646
647 11. Vietor I, Vadivelu SK, Wick N, Hoffman R, Cotten M, Seiser C*, et al.* TIS7 interacts with the
648 mammalian SIN3 histone deacetylase complex in epithelial cells. *Embo J* 2002, **21**(17)**:** 4621-
649 4631.

650
651 12. Wick N, Schleiffer A, Huber LA, Vietor I. Inhibitory effect of TIS7 on Sp1-C/EBPalpha transcription
652 factor module activity. *J Mol Biol* 2004, **336**(3)**:** 589-595.

653
654 13. Park G, Horie T, Kanayama T, Fukasawa K, Iezaki T, Onishi Y*, et al.* The transcriptional modulator
655 Ifrd1 controls PGC-1alpha expression under short-term adrenergic stimulation in brown
656 adipocytes. *The FEBS journal* 2017, **284**(5)**:** 784-795.

657
658 14. Lammirato A, Patsch K, Feiereisen F, Maly K, Nofziger C, Paulmichl M*, et al.* TIS7 induces
659 transcriptional cascade of methylosome components required for muscle differentiation. *BMC*
660 *Biol* 2016, **14**(1)**:** 95.

661
662 15. Latif F, Duh FM, Bader S, Sekido Y, Li H, Geil L*, et al.* The human homolog of the rodent
663 immediate early response genes, PC4 and TIS7, resides in the lung cancer tumor suppressor
664 gene region on chromosome 3p21. *Hum Genet* 1997, **99**(3)**:** 334-341.

665
666 16. Brown A, Baird MR, Yip MC, Murray J, Shao S. Structures of translationally inactive mammalian
667 ribosomes. *Elife* 2018, **7**.

668
669 17. Marcon BH, Holetz FB, Eastman G, Origa-Alves AC, Amoros MA, de Aguiar AM*, et al.*
670 Downregulation of the protein synthesis machinery is a major regulatory event during early
671 adipogenic differentiation of human adipose-derived stromal cells. *Stem Cell Res* 2017, **25:** 191-
672 201.

673
674 18. Farmer SR. Transcriptional control of adipocyte formation. *Cell Metab* 2006, **4**(4)**:** 263-273.

675
676 19. Wang Y, Sul HS. Pref-1 regulates mesenchymal cell commitment and differentiation through
677 Sox9. *Cell Metab* 2009, **9**(3)**:** 287-302.

678
679 20. Kim KA, Kim JH, Wang Y, Sul HS. Pref-1 (preadipocyte factor 1) activates the MEK/extracellular
680 signal-regulated kinase pathway to inhibit adipocyte differentiation. *Mol Cell Biol* 2007, **27**(6)**:**
681 2294-2308.

682
683 21. Lefterova MI, Zhang Y, Steger DJ, Schupp M, Schug J, Cristancho A*, et al.* PPARgamma and C/EBP
684 factors orchestrate adipocyte biology via adjacent binding on a genome-wide scale. *Genes Dev*
685 2008, **22**(21)**:** 2941-2952.

686
687 22. Lowell BB. PPARgamma: an essential regulator of adipogenesis and modulator of fat cell
688 function. *Cell* 1999, **99**(3)**:** 239-242.

689
690 23. Ross SE, Hemati N, Longo KA, Bennett CN, Lucas PC, Erickson RL*, et al.* Inhibition of adipogenesis
691 by Wnt signaling. *Science* 2000, **289**(5481)**:** 950-953.

692
693 24. van Tienen FH, Laeremans H, van der Kallen CJ, Smeets HJ. Wnt5b stimulates adipogenesis by
694 activating PPARgamma, and inhibiting the beta-catenin dependent Wnt signaling pathway
695 together with Wnt5a. *Biochem Biophys Res Commun* 2009, **387**(1)**:** 207-211.

696
697 25. Li HX, Luo X, Liu RX, Yang YJ, Yang GS. Roles of Wnt/beta-catenin signaling in adipogenic
698 differentiation potential of adipose-derived mesenchymal stem cells. *Mol Cell Endocrinol* 2008,
699 **291**(1-2)**:** 116-124.

700
701 26. Tontonoz P, Spiegelman BM. Fat and beyond: the diverse biology of PPARgamma. *Annu Rev*
702 *Biochem* 2008, **77:** 289-312.

703
704 27. Xu C, Wang J, Zhu T, Shen Y, Tang X, Fang L*, et al.* Cross-Talking Between PPAR and WNT
705 Signaling and its Regulation in Mesenchymal Stem Cell Differentiation. *Curr Stem Cell Res Ther*
706 2016, **11**(3)**:** 247-254.

707
708 28. Mortensen SB, Jensen CH, Schneider M, Thomassen M, Kruse TA, Laborda J*, et al.* Membrane-
709 tethered delta-like 1 homolog (DLK1) restricts adipose tissue size by inhibiting preadipocyte
710 proliferation. *Diabetes* 2012, **61**(11)**:** 2814-2822.

711
712 29. Moon YS, Smas CM, Lee K, Villena JA, Kim KH, Yun EJ*, et al.* Mice lacking paternally expressed
713 Pref-1/Dlk1 display growth retardation and accelerated adiposity. *Mol Cell Biol* 2002, **22**(15)**:**
714 5585-5592.

715

716 30. Barclay JL, Nelson CN, Ishikawa M, Murray LA, Kerr LM, McPhee TR*, et al.* GH-dependent STAT5
717 signaling plays an important role in hepatic lipid metabolism. *Endocrinology* 2011, **152**(1)**:** 181-
718 192.

719
720 31. Paul C, Sardet C, Fabbrizio E. The Wnt-target gene Dlk-1 is regulated by the Prmt5-associated
721 factor Copr5 during adipogenic conversion. *Biol Open* 2015, **4**(3)**:** 312-316.

722
723 32. LeBlanc SE, Konda S, Wu Q, Hu YJ, Oslowski CM, Sif S*, et al.* Protein arginine methyltransferase 5
724 (Prmt5) promotes gene expression of peroxisome proliferator-activated receptor gamma2
725 (PPARgamma2) and its target genes during adipogenesis. *Mol Endocrinol* 2012, **26**(4)**:** 583-597.

726
727 33. Sul HS. Minireview: Pref-1: role in adipogenesis and mesenchymal cell fate. *Mol Endocrinol*
728 2009, **23**(11)**:** 1717-1725.

729
730 34. Paul C, Sardet C, Fabbrizio E. The histone- and PRMT5-associated protein COPR5 is required for
731 myogenic differentiation. *Cell Death Differ* 2012, **19**(5)**:** 900-908.

732
733 35. Ruiz-Ojeda FJ, Ruperez AI, Gomez-Llorente C, Gil A, Aguilera CM. Cell Models and Their
734 Application for Studying Adipogenic Differentiation in Relation to Obesity: A Review. *Int J Mol Sci*
735 2016, **17**(7).

736
737 36. Wang S, Sun Z, Zhang X, Li Z, Wu M, Zhao W*, et al.* Wnt1 positively regulates CD36 expression
738 via TCF4 and PPAR-gamma in macrophages. *Cell Physiol Biochem* 2015, **35**(4)**:** 1289-1302.

739
740 37. Prestwich TC, Macdougald OA. Wnt/beta-catenin signaling in adipogenesis and metabolism. *Curr*
741 *Opin Cell Biol* 2007, **19**(6)**:** 612-617.

742
743 38. Lee YL, Helman L, Hoffman T, Laborda J. dlk, pG2 and Pref-1 mRNAs encode similar proteins
744 belonging to the EGF-like superfamily. Identification of polymorphic variants of this RNA.
745 *Biochim Biophys Acta* 1995, **1261**(2)**:** 223-232.

746
747 39. Garces C, Ruiz-Hidalgo MJ, Bonvini E, Goldstein J, Laborda J. Adipocyte differentiation is
748 modulated by secreted delta-like (dlk) variants and requires the expression of membrane-
749 associated dlk. *Differentiation* 1999, **64**(2)**:** 103-114.

750
751 40. Lee K, Villena JA, Moon YS, Kim KH, Lee S, Kang C*, et al.* Inhibition of adipogenesis and
752 development of glucose intolerance by soluble preadipocyte factor-1 (Pref-1). *J Clin Invest* 2003,
753 **111**(4)**:** 453-461.

754
755 41. Coburn CT, Knapp FF, Jr., Febbraio M, Beets AL, Silverstein RL, Abumrad NA. Defective uptake
756 and utilization of long chain fatty acids in muscle and adipose tissues of CD36 knockout mice. *J*
757 *Biol Chem* 2000, **275**(42)**:** 32523-32529.

758

759 42. Wilson CG, Tran JL, Erion DM, Vera NB, Febbraio M, Weiss EJ. Hepatocyte-Specific Disruption of
760 CD36 Attenuates Fatty Liver and Improves Insulin Sensitivity in HFD-Fed Mice. *Endocrinology*
761 2016, **157**(2)**:** 570-585.

762
763 43. Koliwad SK, Streeper RS, Monetti M, Cornelissen I, Chan L, Terayama K*, et al.* DGAT1-dependent
764 triacylglycerol storage by macrophages protects mice from diet-induced insulin resistance and
765 inflammation. *J Clin Invest* 2010, **120**(3)**:** 756-767.

766
767 44. Cases S, Smith SJ, Zheng YW, Myers HM, Lear SR, Sande E*, et al.* Identification of a gene
768 encoding an acyl CoA:diacylglycerol acyltransferase, a key enzyme in triacylglycerol synthesis.
769 *Proc Natl Acad Sci U S A* 1998, **95**(22)**:** 13018-13023.

770
771 45. Ludwig EH, Mahley RW, Palaoglu E, Ozbayrakci S, Balestra ME, Borecki IB*, et al.* DGAT1 promoter
772 polymorphism associated with alterations in body mass index, high density lipoprotein levels
773 and blood pressure in Turkish women. *Clin Genet* 2002, **62**(1)**:** 68-73.

774
775 46. Tsai J, Qiu W, Kohen-Avramoglu R, Adeli K. MEK-ERK inhibition corrects the defect in VLDL
776 assembly in HepG2 cells: potential role of ERK in VLDL-ApoB100 particle assembly. *Arterioscler*
777 *Thromb Vasc Biol* 2007, **27**(1)**:** 211-218.

778
779 47. Gautam J, Khedgikar V, Kushwaha P, Choudhary D, Nagar GK, Dev K*, et al.* Formononetin, an
780 isoflavone, activates AMP-activated protein kinase/beta-catenin signalling to inhibit
781 adipogenesis and rescues C57BL/6 mice from high-fat diet-induced obesity and bone loss. *Br J*
782 *Nutr* 2017, **117**(5)**:** 645-661.

783
784 48. Bennett CN, Hodge CL, MacDougald OA, Schwartz J. Role of Wnt10b and C/EBPalpha in
785 spontaneous adipogenesis of 243 cells. *Biochem Biophys Res Commun* 2003, **302**(1)**:** 12-16.

786
787 49. Christiaens V, Van Hul M, Lijnen HR, Scroyen I. CD36 promotes adipocyte differentiation and
788 adipogenesis. *Biochim Biophys Acta* 2012, **1820**(7)**:** 949-956.

789
790 50. Nagasaka H, Yorifuji T, Takatani T, Okano Y, Tsukahara H, Yanai H*, et al.* CD36 deficiency
791 predisposing young children to fasting hypoglycemia. *Metabolism* 2011, **60**(6)**:** 881-887.

792
793 51. Kashiwagi H, Tomiyama Y, Nozaki S, Kiyoi T, Tadokoro S, Matsumoto K*, et al.* Analyses of genetic
794 abnormalities in type I CD36 deficiency in Japan: identification and cell biological
795 characterization of two novel mutations that cause CD36 deficiency in man. *Hum Genet* 2001,
796 **108**(6)**:** 459-466.

797
798 52. Glazier AM, Scott J, Aitman TJ. Molecular basis of the Cd36 chromosomal deletion underlying
799 SHR defects in insulin action and fatty acid metabolism. *Mamm Genome* 2002, **13**(2)**:** 108-113.

800

801 53. Tanaka T, Nakata T, Oka T, Ogawa T, Okamoto F, Kusaka Y*, et al.* Defect in human myocardial
802 long-chain fatty acid uptake is caused by FAT/CD36 mutations. *J Lipid Res* 2001, **42**(5)**:** 751-759.

803
804 54. Neeland IJ, Ayers CR, Rohatgi AK, Turer AT, Berry JD, Das SR*, et al.* Associations of visceral and
805 abdominal subcutaneous adipose tissue with markers of cardiac and metabolic risk in obese
806 adults. *Obesity (Silver Spring)* 2013, **21**(9)**:** E439-447.

807
808 55. Lemonnier D. Effect of age, sex, and sites on the cellularity of the adipose tissue in mice and rats
809 rendered obese by a high-fat diet. *J Clin Invest* 1972, **51**(11)**:** 2907-2915.

810
811 56. Popow J, Alleaume AM, Curk T, Schwarzl T, Sauer S, Hentze MW. FASTKD2 is an RNA-binding
812 protein required for mitochondrial RNA processing and translation. *RNA* 2015, **21**(11)**:** 1873-
813 1884.

814
815 57. Shore P, Dietrich W, Corcoran LM. Oct-2 regulates CD36 gene expression via a consensus
816 octamer, which excludes the co-activator OBF-1. *Nucleic Acids Res* 2002, **30**(8)**:** 1767-1773.

817
818 58. Reintjes A, Fuchs JE, Kremser L, Lindner HH, Liedl KR, Huber LA*, et al.* Asymmetric arginine
819 dimethylation of RelA provides a repressive mark to modulate TNFalpha/NF-kappaB response.
820 *Proc Natl Acad Sci U S A* 2016, **113**(16)**:** 4326-4331.

821

822

Vietor_Figure 1

a

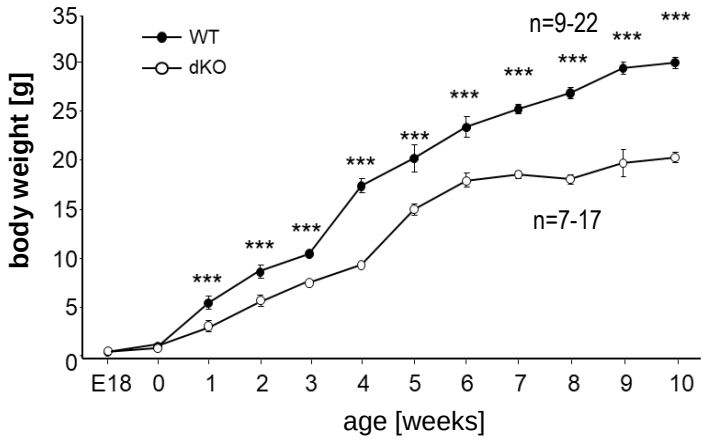

b

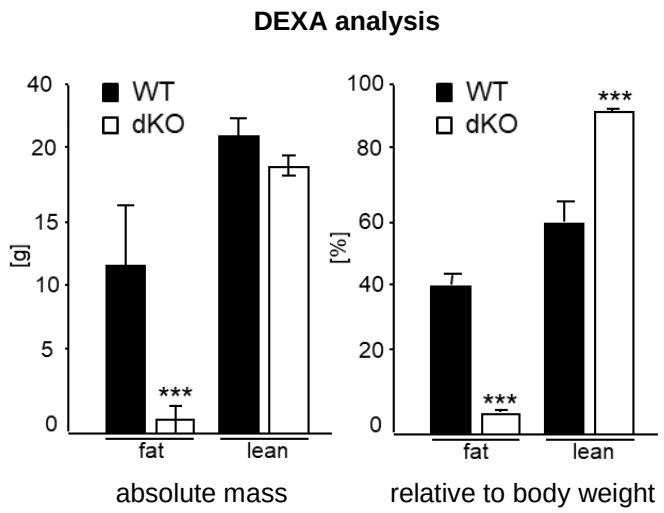

c

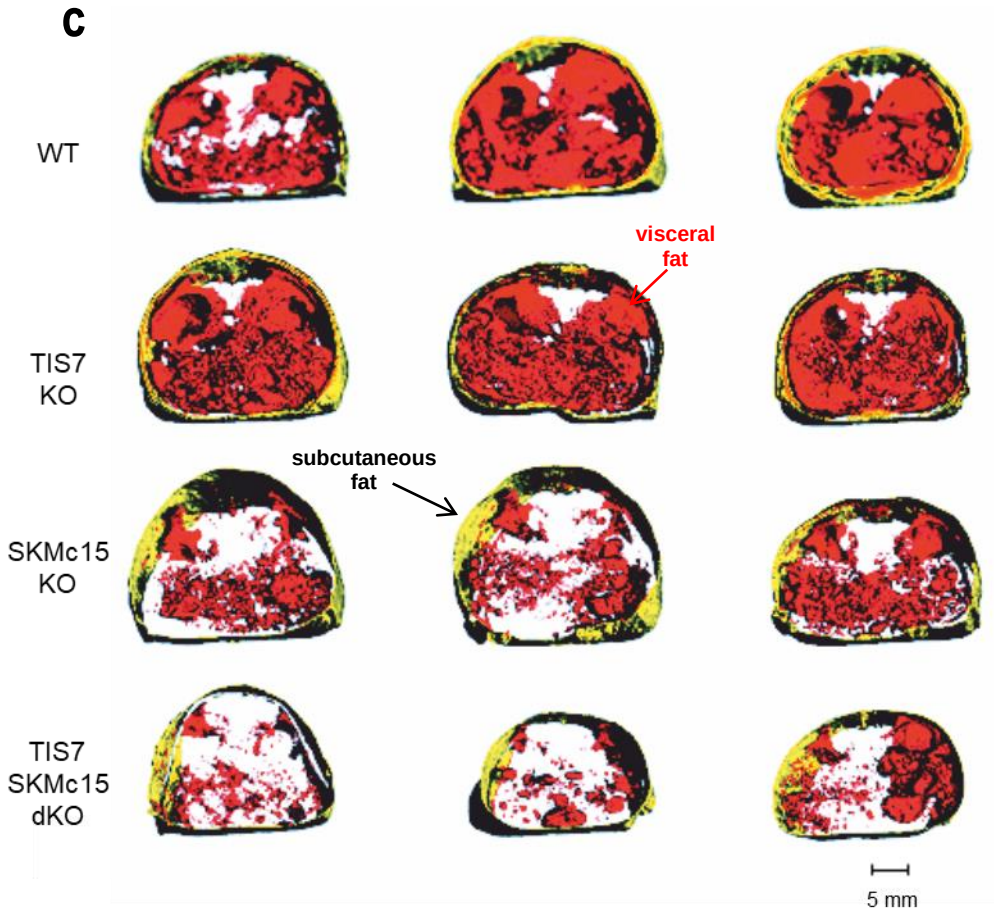

Vietor_Figure 2

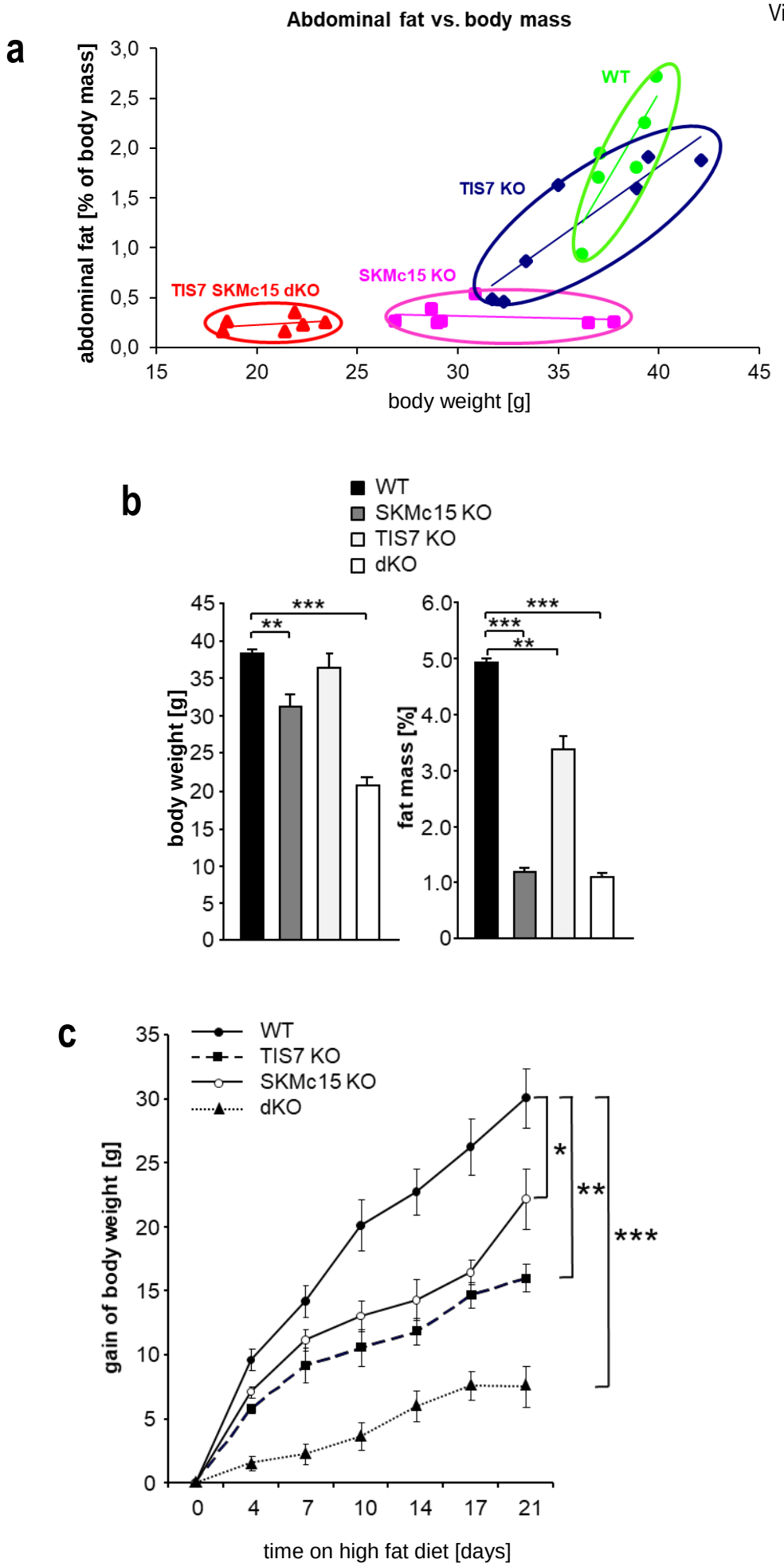

Vietor_Figure 3

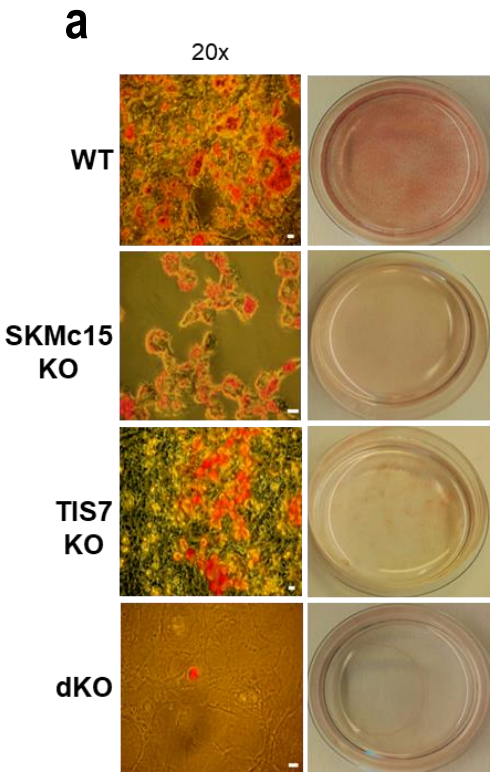

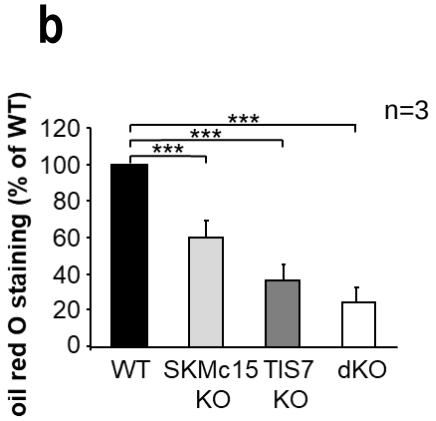

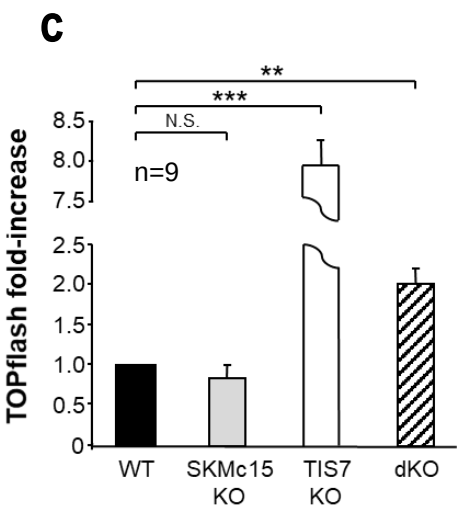

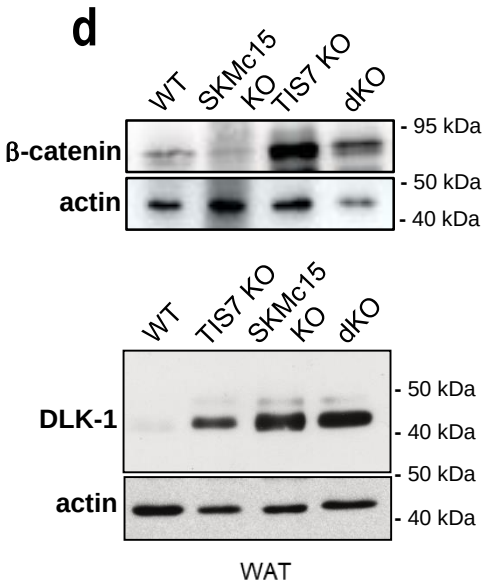

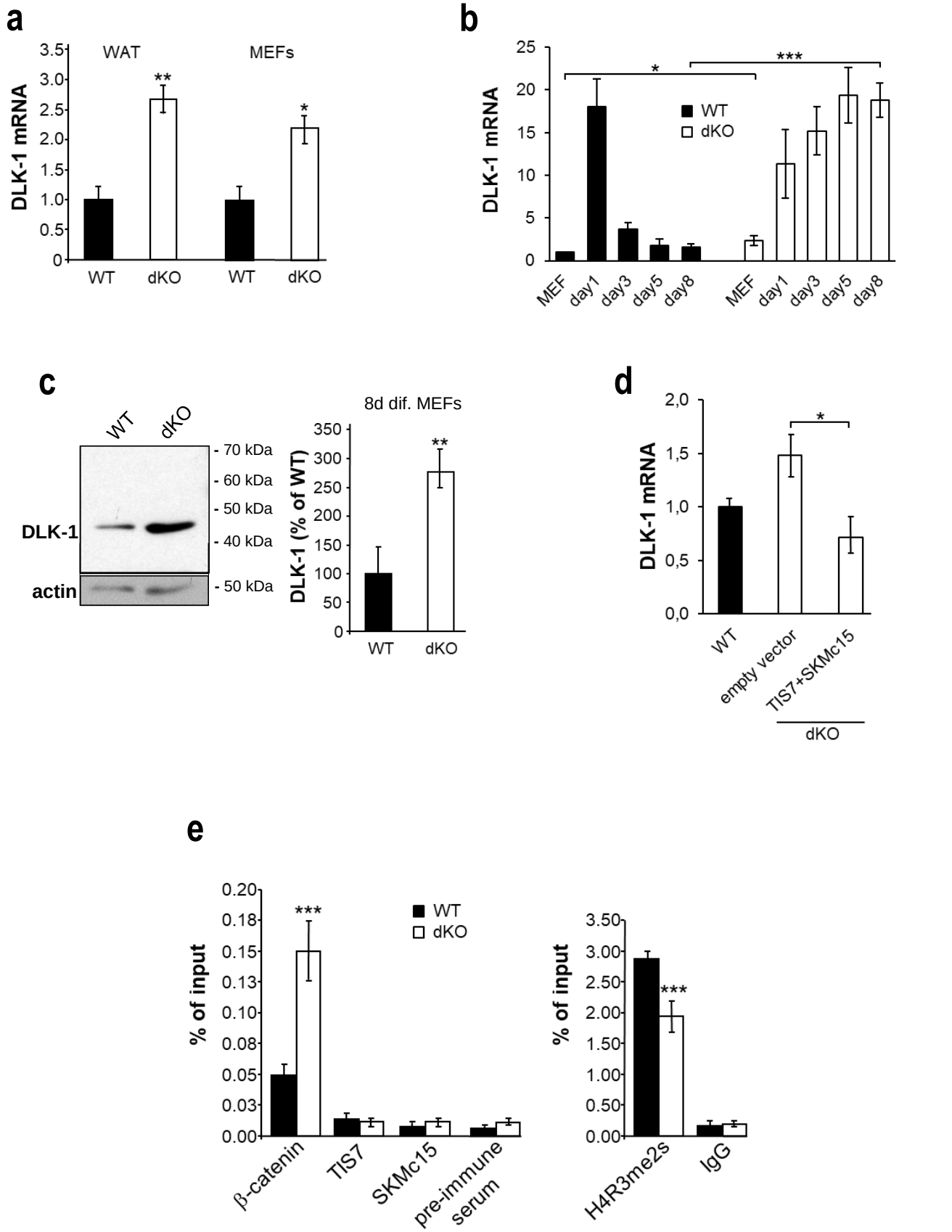
a
WAT
MEFs
DLK-1 mRNA
3.5
3.0
2.5
2.0
1.5
1.0
0.5
0
**
*
WT
dKO
WT
dKO
b
DLK-1 mRNA
25
20
15
10
5
0
*
***
WT
dKO
MEF
day1
day3
day5
day8
MEF
day1
day3
day5
day8
c
WT
dKO
DLK-1
actin
70 kDa
60 kDa
50 kDa
40 kDa
50 kDa
8d dif. MEFs
DLK-1 (% of WT)
350
300
250
200
150
100
50
0
**
WT
dKO
d
DLK-1 mRNA
2,0
1,5
1,0
0,5
0,0
*
WT
empty vector
TIS7+SKMc15
dKO
e
% of input
0.20
0.18
0.15
0.13
0.10
0.08
0.05
0.03
0.00
***
WT
dKO
β-catenin
TIS7
SKMc15
pre-immune serum
% of input
3.50
3.00
2.50
2.00
1.50
1.00
0.50
0.00
***
H4R3me2s
IgG

Vietor_Figure 5

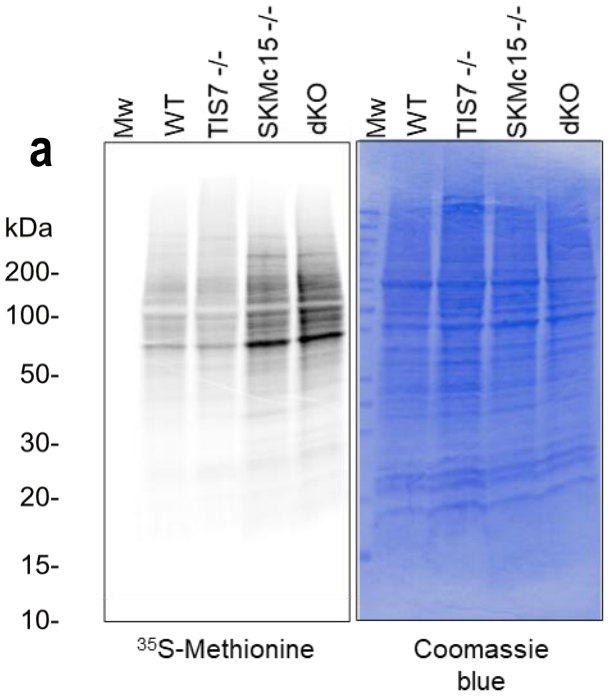

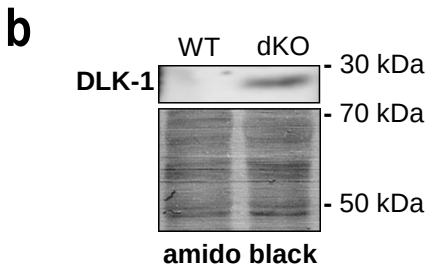

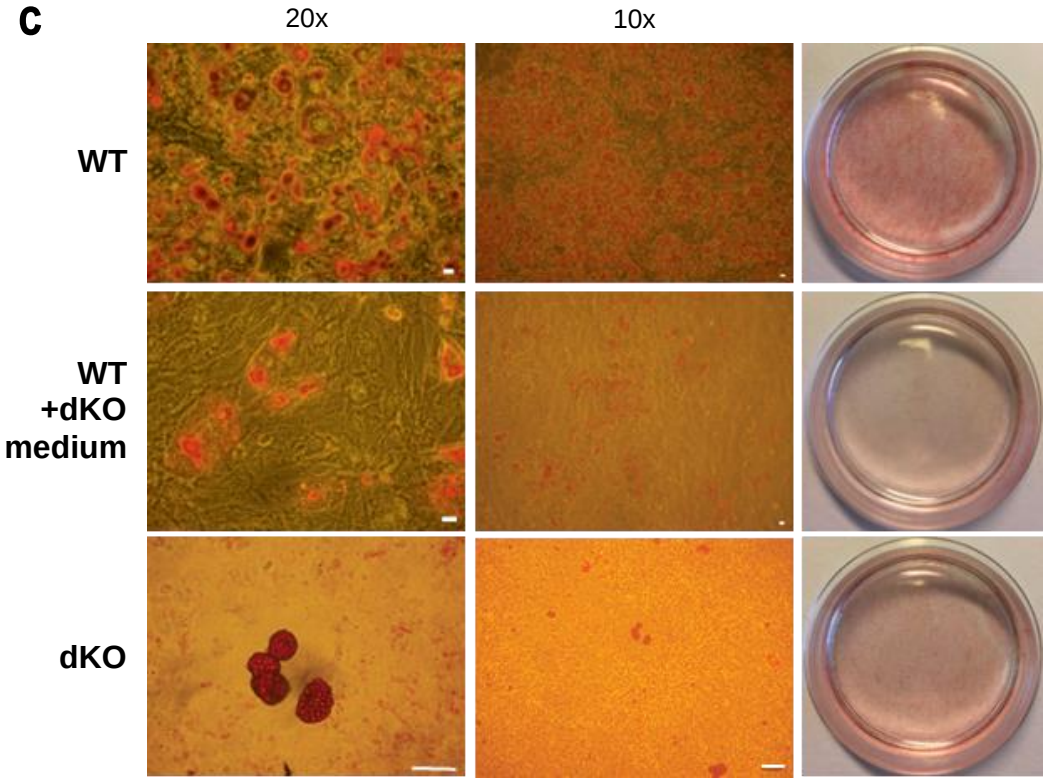

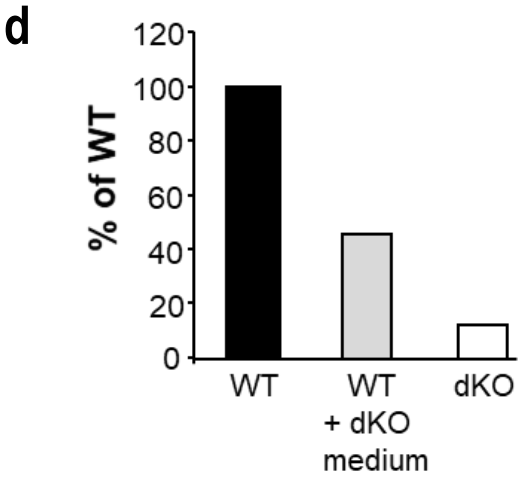

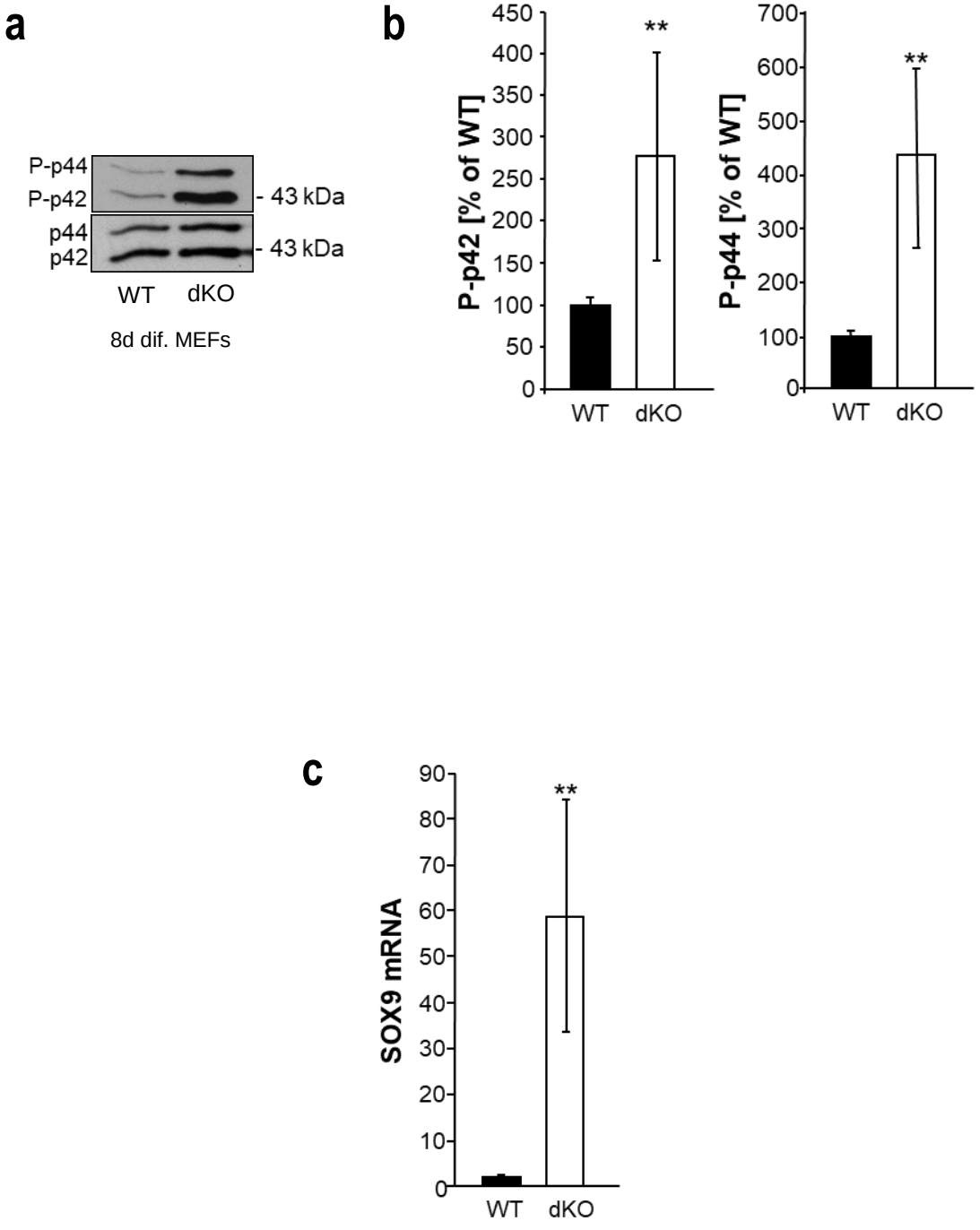
a
P-p44
P-p42
- 43 kDa
p44
p42
- 43 kDa
WT
dKO
8d dif. MEFs
b
P-p42 [% of WT]
450
400
350
300
250
200
150
100
50
0
**
WT
dKO
P-p44 [% of WT]
700
600
500
400
300
200
100
0
**
WT
dKO
c
SOX9 mRNA
90
80
70
60
50
40
30
20
10
0
**
WT
dKO

Vietor_Figure 7

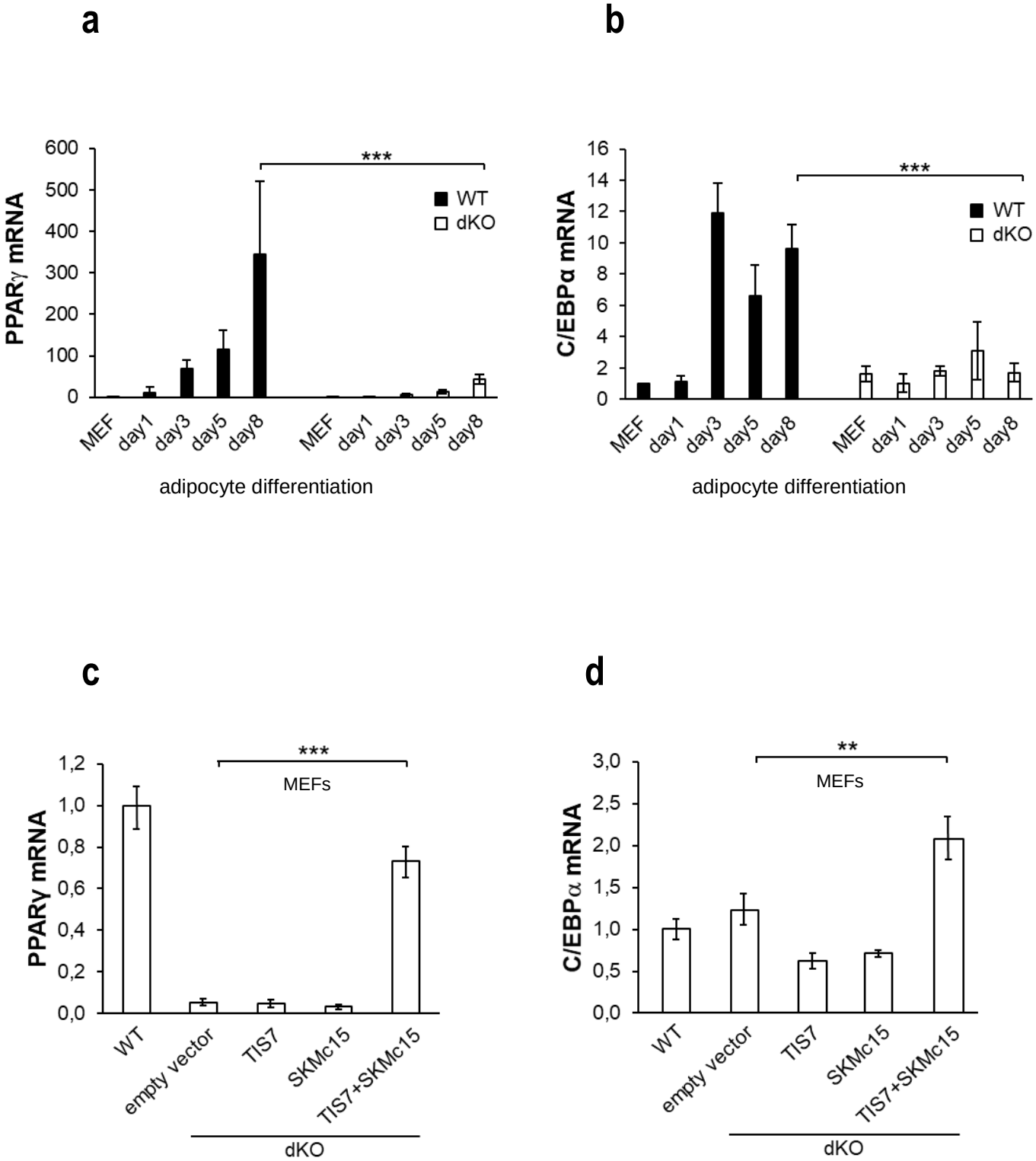

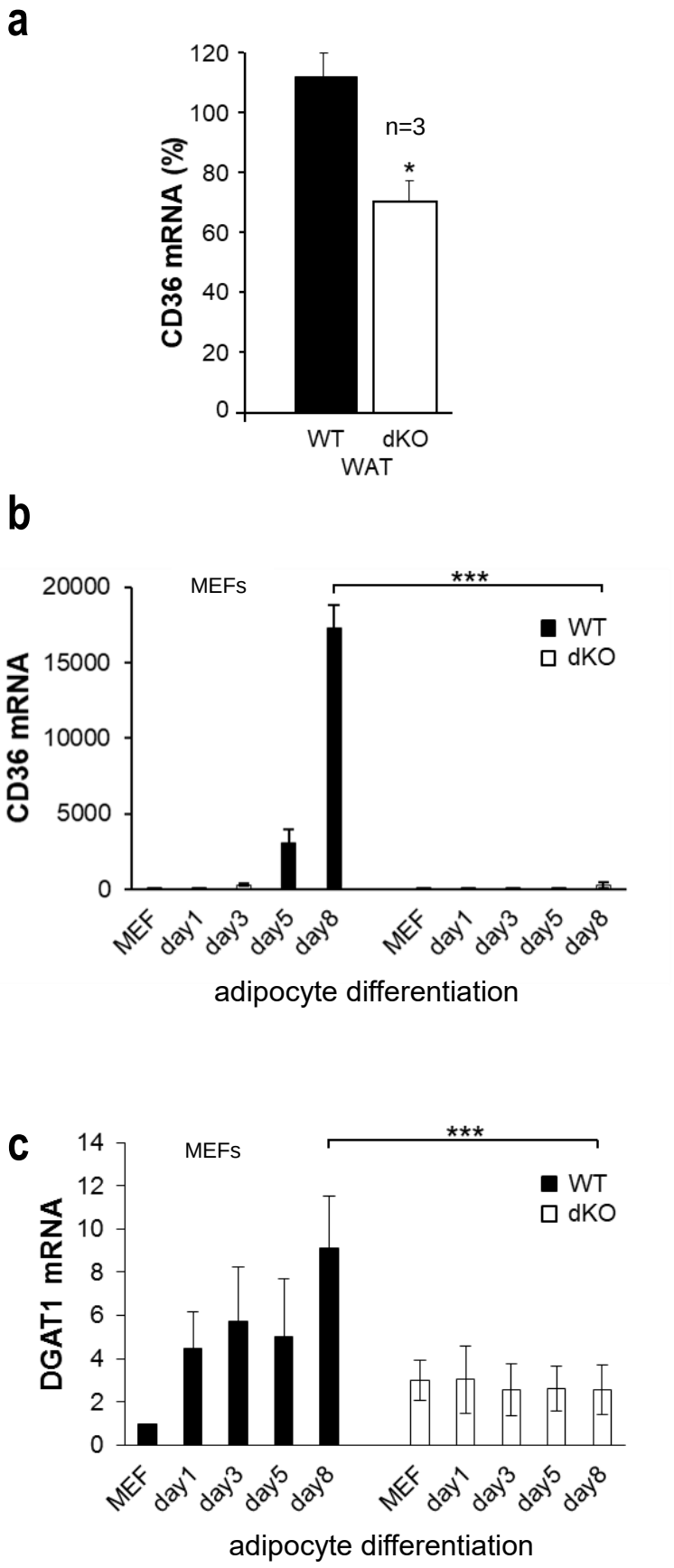
a
CD36 mRNA (%)
120
100
80
60
40
20
0
n=3
*
WT
dKO
WAT
b
CD36 mRNA
20000
15000
10000
5000
0
MEFs
***
WT
dKO
MEF
day1
day3
day5
day8
adipocyte differentiation
c
DGAT1 mRNA
14
12
10
8
6
4
2
0
MEFs
***
WT
dKO
MEF
day1
day3
day5
day8
adipocyte differentiation
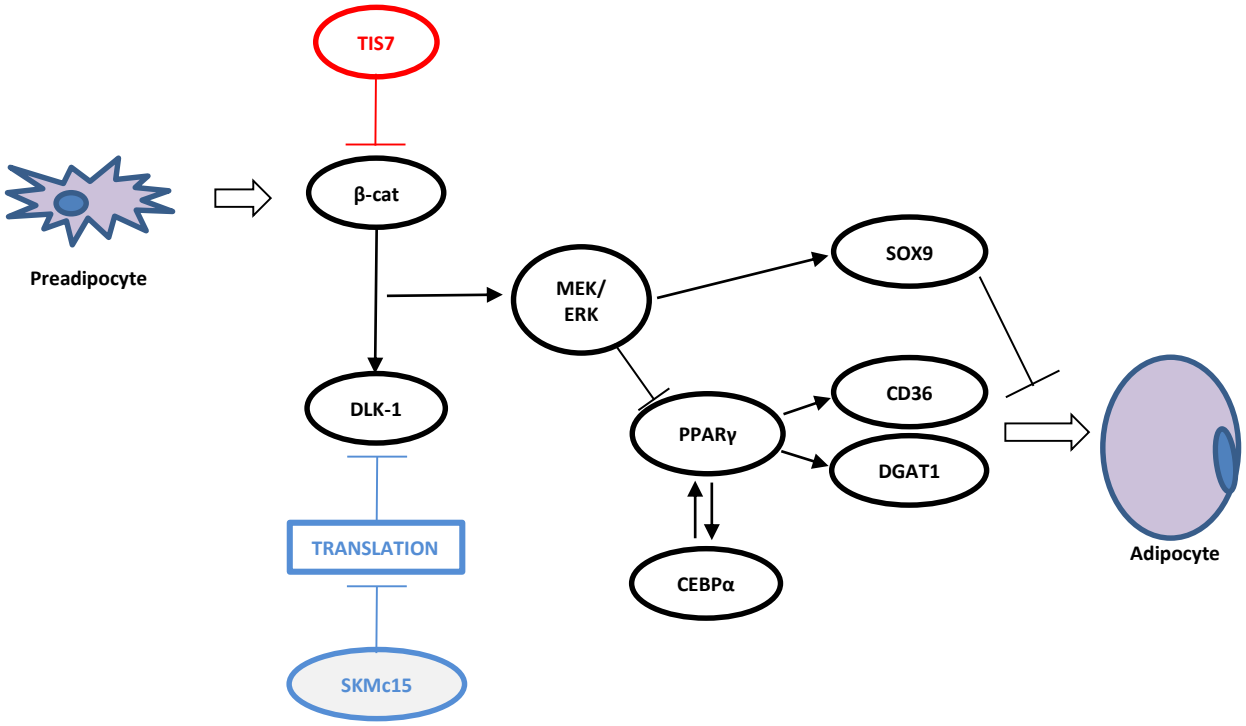
Vietor_Figure 9